University Hospital Tübingen,
Department of General, Visceral and
Transplant Surgery

Development and validation of an *ex vivo* model for optimizing intraperitoneal drug delivery

**Inaugural Dissertation
submitted for a
Doctoral Degree in
Medicine**

**at the
Faculty of Medicine
Eberhard Karls Universität
Tübingen**

**Submitted by
Sautkin, Iaroslav**

2022

Dean: Professor Dr. B. Pichler
First Reviewer: Professor Dr. A. Königsrainer
Second Reviewer: Professor Dr. S. Beckert

Date of the defense: 13.09.2022

Table of Contents

List of tables

List of figures

List of Abbreviations

AIN	angiogenesis inhibitors
ANOVA	analysis of variance
AAS	atom absorption spectroscopy
ARRIVE	animal research: reporting of in vivo experiments
CA-125	cancer antigen 125
CA19-9	cancer antigen 19-9
CAT	computerized axial tomography
CAWS	closed air waste system
CEA	carcinoembryonic antigen
CI	confidential interval
Cis	cisplatin
CQA	critical quality attribute
CRS	cytoreductive surgery
CT	computed tomography
CUP	Carcinoma of unknown primary
Dbait	DNA repair inhibitor
Dbait-Cy5	Dbait coupled with cyanine
DL	diagnostic laparoscopy
DNA	deoxyribonucleic acid
Dox	doxorubicin
eIBUB	enhanced IBUB
EGF	epidermal growth factor

EPIC	early postoperative intraperitoneal chemotherapy
ePIPAC	electrostatic PIPAC
GL-ONC	modified oncolytic vaccinia virus
HEPA	high-efficiency particulate absorbing filter
HIPEC	hyperthermic intraperitoneal chemotherapy
HPC	hermetic plastic cup
hPIPAC	hyperthermic PIPAC
HPLC	high performance liquid chromatography
IBUB	inverted bovine urinary bladder
ID	identification number
IL-1	interleukin 1
IL-1b	interleukin 1b
INF-γ	interferon gamma
LLoQ	low level of quantification
MKN45	human gastric adenocarcinoma cell line
MR	magnetic resonance imaging
NMR	nuclear magnetic resonance

PCI	peritoneal carcinomatosis index
PET	positron emission tomography
PIPAC	pressurized intraperitoneal aerosol chemotherapy
PM	peritoneal metastasis
PRGS	peritoneal regression grading score
R&D	research and development
SKOV3	human ovarian carcinoma cell line
SPECT	single-photon-emissions-tomographie
TNF-α	tumor necrosis factor-alpha
TGF-β	transforming growth factor-beta
VX2	rabbit anaplastic squamous cancer cell line
VGA	video graphics array
usPIPAC	ultrasound PIPAC

1 Introduction

1.1 Peritoneal anatomy and physiology

The peritoneum is a serous membrane consisting of a layer of mesothelial cells lining the abdominal wall and viscera [1]. The abdominal cavity as one of the three serous cavities in the human body was described by Bichat in 1813 [2], and in 1890 Minot described the mesothelium or coelom as an epithelial membrane of the embryonic serosal cavity [3]. The peritoneal cavity development begins in the gastrulation phase of embryogenesis, when three primary germ layers, the ectoderm, the mesoderm, and the endoderm, develop. Later on, the mesoderm splits into the somatic and the splanchnic layers, which further differentiate into parietal and visceral layers [4] with a joint surface over 1.4 m^2 [5, 6]. The parietal peritoneum lines the abdominal wall, the

visceral peritoneum covers the abdominal organs [1]. The space between the two layers is defined as the peritoneal cavity [7] and usually contains 50-75 ml serous fluid [8]. Another serous organ is the greater omentum, formed from two mesothelial sheets enveloping adipocytes [9]. The greater omentum is located anterior to the stomach and posterior to the transverse colon [10]. The weight of the greater omentum varies from 300 to 2000 g with a surface of 300 to 1500 cm^2 [11].

In the adult, the peritoneal serosa consists of mesothelial cells with surface microvilli [12], a basal membrane, and supporting connective tissue. These structures are supplied by blood and lymph vessels in the subperitoneal layer (Figure 1, Figure 2) [13]. Many capillaries are directly under the serosa, which are termed omental glomeruli due to their similarity to the renal glomeruli [14]. Around the omental

glomeruli are aggregates of leucocytes supported by tiny reticular fibres [15]. These aggregates, called "milky spots", include macrophages, B-lymphocytes, T-lymphocytes, mast cells, and stromal cells [16].

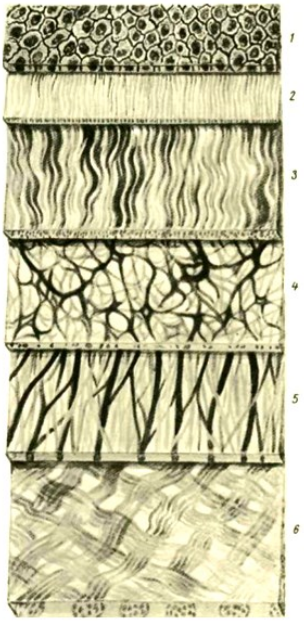

***Figure 1*: Anatomy of the peritoneum.**
The layered structure of the peritoneum [4], consists of 1) Mesothelium (2.5-3 µm), 2) basal membrane (0.8-1.0 µm), 3) superficial wavy collagen layer, 4) superficial diffuse elastic net, 5) deep longitudinal elastic net, 6) collagen-elastic layer.

The parietal peritoneum covers 30%, the visceral peritoneum covers 70% of the total peritoneal surface area [17]. The blood supply to the human peritoneum comprises 1%-2% of the cardiac minute volume [17], or 60-100 ml per minute [18]. *In vivo* studies in the cat demonstrated that the parietal layer receives a blood flow of around 6.2 ± 1.2 ml per min per 100 g tissue. The parietal peritoneum is perfused by the intercostal, epigastric, circumflex, iliac, and lumbar arteries. The visceral layer receives a blood flow of approximately 9.7 ± 1.9 ml per min per 100 g [19]. The vasculature of the visceral peritoneum derives from the tr. coeliacus and the aa. mesenterica superior and inferior [20].

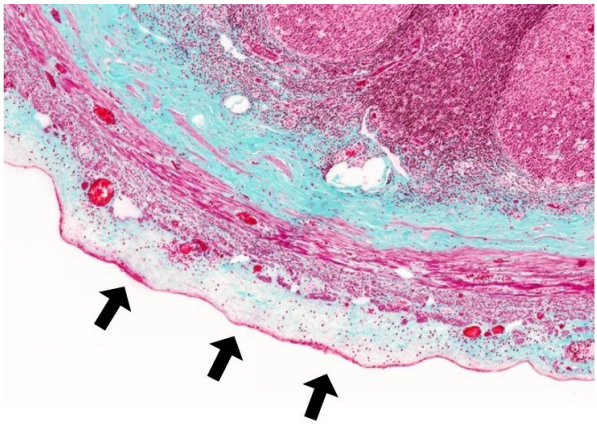

***Figure 2*: Cross section of the human appendix vermiformis.**
Typical 5-layered structure of a digestive organ, covered by a layer of mesothelial cells, the peritoneum (arrows), Masson-Goldner staining [21]. Reproduced with permission from [21].

- Peritoneal absorption

The peritoneum can resorb a substantial fluid volume rapidly. The fluid transport through the serosal cavity is facilitated by microvilli, which increase the peritoneal surface considerably. Moreover, the microvilli are covered with glycosaminoglycans that contribute to absorption (see below) [22]. The

transmesothelial transport of fluid and molecules occurs through intercellular junctions and lymphatic stomata, micrometer-sized openings ensuring a rapid clearance of larger particles from the peritoneal cavity [23, 24].

- Peritoneal secretion

The peritoneal mesothelium also has a secretion function. The peritoneum is covered by the glycocalyx, a chemical barrier composed of glycosaminoglycans (hyaluronans) and glycoplipids (phosphatidylcholine). The glycocalyx is negatively charged, due to the presence of glycosaminoglycans [25]. The smooth, gliding peritoneal surface prevents friction between peritoneal layers [26], protects the peritoneum from erosion and inflammation, and prevents tumor cell adhesion [27]. At the same time, the peritoneum secretes prostaglandins, which play a decisive role in local pro- and anti-inflammatory processes [28].

Growth factors are secreted by mesothelial cells when the peritoneum is exposed to non-physiological solutions, e.g. during peritoneal dialysis, contributing to the formation of peritoneal adhesions and an increased serosa permeability [29]. Proteoglycans produced by the mesothelium downregulate TGF-β and collagen fibres proliferation. This downregulation prevents the development of fibrosis and peritoneal adhesions [30] and thus, tumor cell anchoring and proliferation. Mesothelial cells have antitumor activity, at least in the early phase of peritoneal tumor spreading [31]. Free hyaluronan released from the glycocalyx binds with tumor CD44 receptors, inhibiting cancer progression [32] and preventing further tumor dissemination through the hyaluronan-covered mesothelium [33].

- Immunological function

The peritoneum is also an immunological organ: antigen presentation by the mesothelium was observed after exposition to the tetanus toxoid and the super antigen *Staphylococcus aureus* α [34]. The mesothelium also has procoagulant and fibrinolytic activities, which play an important role in the healing process after abdominal surgery or bacterial peritonitis [35]. The healing process of the mesothelium initiates within 24 hours after injury. It lasts at least ten days, ending in the best case when the injured site is covered with a reconstituted, functional peritoneum, in the worst case with a scar of connective tissue [36, 37].

1.2 Peritoneal metastasis

1.2.1 Pathophysiology

The term "Peritoneal metastasis" (PM) is defined as the spreading of malignant cells

within the peritoneal cavity and the development of tumor implants on the peritoneal lining [38]. Metastatic dissemination throughout the peritoneal cavity is frequently observed in ovarian, gastric, colorectal, and other gastrointestinal cancers, which often are mucous-rich [39]. The development of PM comprises four phases, namely dissemination, adhesion, invasion, and progression [40]. Most often, tumor dissemination within the abdominal cavity occurs over the transcoelomic pathway. It is unclear if systemic, blood-borne spreading can also give rise to PM [41].

Some authors distinguish between PM and peritoneal recurrence. PM is caused by the exfoliation of primary origin tumor cells with subsequent peritoneal dissemination (tumor-based mechanism). In this scenario, the peritoneal invasion occurs only in the presence of biologically aggressive tumors.

For one century, surgeons know that peritoneal wounds are preferred sites of tumor recurrence. Peritoneal recurrence finds its origin in surgical trauma leading to mechanical spreading of tumor cells and their implantation in surgical wounds. Damage to the glycocalyx and exposition of the basal membrane facilitate cancer cells adhesion. A fibrinous exudate entraps tumor cells at the lesion site, which are further bound with submesothelial connective tissue by integrins [42, 43] and lead to tumor progression. In contrast to PM, peritoneal recurrence can occur in early tumor stages, and also in biologically less aggressive cancer [44].

1.2.2 Symptoms and diagnosis

In the early stages of PM, clinical symptoms and signs are limited, which complicates diagnosis and delays treatment. Along with disease progression, patients develop nausea, diarrhea, abdominal pain, bloating, and weight

loss [45]. Quality of life is deteriorating [46]. In advanced PM stages, complications such as intestinal obstruction or ascites are frequent, leading to the so-called cachexia-anorexia syndrome and, ultimately, death [47].

PM diagnosis is usually by imaging methods such as ultrasound, CT-scan, NMR-scans, and PET/CT [48], but PM can also be discovered during surgery. CT is the most commonly applied method. Despite its frequent use, results are still unsatisfactory [49, 50]. The sensitivity of CT for PM varies between 41% and 93%, with a specificity of 78% to 96% [51]. When the tumor nodule is smaller than 1 cm, CT sensitivity is as low as 25% [52]. CT is commonly used to monitor previously observed abnormalities such as fat and subcapsular metastasis, structural heterogeneity, and nodular lesions [51].

In some abdomen regions, MRI has demonstrated increased accuracy in PM detection vs. CT [53]. However, motion artifacts from bowel peristalsis impair the sensitivity of MRI for PM [50]. As compared with MRI, PET has increased sensitivity but similar limitations [54]. PET-CT does not deliver meaningful metabolic information in mucus-rich tumors. The use of ultrasound in diagnosis of PM originated from ovarian cancer characterized by high sensitivity 81.4-91% and specificity 88-96%. The sensitivity of CAT vs. ultrasound in preoperative staging of ovarian malignancy was 71% vs. 75% [55].

The tumor markers CEA, CA-125, and CA 19-9 have no value in PM's early diagnosis. However, they might play a role in postoperative surveillance and detecting peritoneal recurrence after surgery [56-58]. However, the part of tumor markers in PM is not

well characterized due to the lack of radiological gold standard.

Staging laparoscopy is increasingly used in clinical practice. This procedure allows aspiration of ascitic fluid [59] and tumor sampling for histological diagnosis [60, 61]. In cancers with unknown primary (CUP), laparoscopy can determine the organ of origin (in particular, appendiceal tumors). Biopsies taken during DL allow objective assessment of histological tumor response [61-63]. Whereas DL is feasible in most patients, it cannot be performed in the presence of massive peritoneal thickness or adhesions [61].

Staging laparoscopy is the method of choice for determining the extent of peritoneal dissemination (using the so-called Peritoneal Cancer Index (PCI) [64] staging. PCI is a scoring system for assessing the spread of

metastasis over thirteen predesigned abdominal regions. Each lesion can score 0 to 3 points depending on tumor size, with the maximal number of points totalizing 39 [65]. PCI helps choose the optimal treatment mode for each patient [73] and is a strong predictor of survival [65]. For example, in patients with PM from colon cancer, a PCI higher 20 predicts a 20% five-year survival rate, while no long-term survivors have a PCI lower than 20 [66]. By measuring qualitatively and quantitatively the involvement of different parts of the abdomen, staging laparoscopy defines a possible indication for cytoreductive surgery (CRS) [59]. CRS and hyperthermic intraperitoneal chemotherapy (HIPEC) is indicated for patients with limited peritoneal involvement (PCI < 6 to 8 in gastric PM, PCI < 17-19 in colorectal PM [67]). Patients with a higher PCI are candidates for palliative chemotherapy or best supportive

care. Surgical indications are then limited to symptom relief (e.g. gastrostomy or ostomy) or to treat complications. Palliative surgery in PM does not increase overall survival [68].

Histological assessment of biopsies (sampled during a laparoscopy or open surgery) are required for diagnosing PM. They also help estimate prognosis. At least four millimetric biopsies should be taken to reflect tumor heterogeneity within the abdomen. An additional, centimetric local peritonectomy is recommended to increase sensitivity for isolated tumor cells [69]. The "Peritoneal Regression Grading Score" (PRGS) was proposed to evaluate the histological response of PM to chemotherapy. PRGS is a four-tied score quantifying PM regression from a complete response (absence of tumor cells, PRGS 1) to a vital tumor with no sign of regression (PRGS 4). The PRGS paves the

way to individualized therapy of patients with PM [69].

1.2.3 Treatment

Once perceived a deadly disease with no therapeutic option, PM is currently an intensive research topic. Several therapeutic options can be offered for PM patients, alone, in sequence, or a combination [70]:

- Curative cytoreductive surgery,
- Systemic palliative chemotherapy, including targeted agents,
- Intraperitoneal chemotherapy (HIPEC, PIPAC, EPIC, etc.),
- Systemic or locoregional immunotherapy, including Intraperitoneal cytolytic virotherapy,
- Endoscopic procedures (dilatation, stent, discharge tubing, etc.),
- Palliative surgery (bypass, ostomy, etc.).

Systemic palliative chemotherapy significantly improves the prognosis of metastatic cancer [71] and is thus proposed to most PM patients [72, 73]. Depending on PM origin, platin-based, anthracycline- and taxane-based regimens are recommended [74]. Angiogenesis inhibitors such as bevacizumab are widely used in patients with PM of ovarian [75] and colorectal [76] origin. Angiogenesis inhibitors are endogenous substances with a broad spectrum of effects, including but not limited to vessel growth inhibition. *In vivo* and *ex vivo* studies have demonstrated that angiogenesis inhibitors can affect tumor vasculature proliferation [77-79]. Some angiogenesis inhibitors, such as angiostatin, endostatin, and serpin protease nexin-1, specifically inhibit proliferating endothelial cells in forming blood vessels [80-82]. Systemic chemotherapy improves the outcome of patients with PM, in particular, in the

upfront situation. However, compared to liver or lung metastasis, PM is relatively resistant to systemic chemotherapy [83].

Intraperitoneal administration of angiogenesis inhibitors in animal models effectively suppressed PM growth [84, 85]. Clinical data are limited with a single trial in 53 patients with PM of gastrointestinal origin: intraperitoneal bevacizumab was well tolerated. Still, it did not result in significantly better control of malignant ascites [86].

Cytoreductive surgery (CRS) is the only potentially curative therapy for PM. To be effective, CRS requires the complete resection of macroscopic tumor nodules (so-called CC-0) [87]. The surgeon first examines the abdominal cavity and determines the feasibility of complete tumor resection. If possible, all macroscopic tumor sites are then removed.

Complete CRS frequently requires multiple resections since the visceral peritoneum can not be stripped from the underlying organ. Thus, CRS is an aggressive and longer procedure with significant morbidity and mortality [88, 89]. CRS usually necessitates intensive care therapy [89], and impairs quality of life for about one year [90].

The high recurrence rate after CRS (up to 80% one year after CRS for colorectal cancer) has let some authors distribute heated liquid chemotherapy (Hyperthermic IntraPEritoneal Chemotherapy, HIPEC) into the peritoneal cavity immediately after CRS [91, 92]. The principle of HIPEC is creating a synergy between chemical and thermal cytotoxicity. A cytotoxic effect of hyperthermia alone was demonstrated *in vitro* at a temperature of 42.5 ºC. Hyperthermia increases the antitumor effect of selected chemotherapeutics (for example,

oxaliplatin, mitomycin, doxorubicin, and cisplatin) and enhances drug penetration into the tissue [93]. In ovarian cancer patients pretreated with neoadjuvant chemotherapy, adding HIPEC to CRS significantly increased overall survival [94]. However, the PRODIGE-7 trial in colorectal cancer patients, whereas confirming an exceptionally median survival after CRS with 41-43 months, did not show any additional advantage of HIPEC vs. CRS alone [95].

Another means of intraperitoneal chemotherapy is early postoperative intraperitoneal chemotherapy (EPIC). EPIC is delivered over a catheter placed during surgery and allows the continuous application of cytostatics for several days after surgery. EPIC has the advantages of repeating chemotherapy application and prolonging the exposure of tumor cells to cytostatics. EPIC is not combined

with hyperthermia. However, like HIPEC, EPIC is also associated with significant mortality and morbidity [96].

Palliative surgery offers limited options in advanced cancer patients, in particular, in the presence of bowel obstruction [97]. The surgical indication is to relieve symptoms and improve quality of life [98, 99]. However, such palliative procedures in PM are challenging due to the patient's cachectic condition and disease's diffuse nature, so that they frequently have a poor outcome [100, 101].

Intraperitoneal immunotherapy is a promising approach in the treatment of PM [102]. Since cancer-associated immunosuppression can be reversible [103], the application of immunostimulating substances (such as cytokines, Toll-like receptor ligands, etc.) is a reasonable approach [104, 105]. Previous studies of vaccine-based therapies, adoptive

cell transfer, immune checkpoint inhibitors, and chimeric T cells with tumor-specific antigen receptors showed promising results for controlling tumor spread and stimulation of antitumor immunity [106-109]. New approaches increase immune cells' specificity, and strategies combining chemotherapy with cytokines, growth factors, and polyvalent vaccines are coming up [110-112].

Finally, several laboratory and clinical studies have demonstrated the potential of oncolytic virotherapy in treating peritoneal cancer. Oncolytic viruses can selectively affect tumor cells without harming normal tissue [113, 114]. Furthermore, they can stimulate the antitumor immune response to neoantigens and the inflamed tumor microenvironment [115]. Systemic virotherapy has limitations related to low viral concentration in the target tissue and the host immune response [116]. The

locoregional application of oncolytic vaccines could overcome these constraints [117, 118]. A Phase I Study with the oncolytic vaccinia virus GL-ONC1 showed the feasibility and safety of intraperitoneal cytolytic virotherapy. This study delivered the first proof of principle of efficacy for treating PM [119]. Combining virotherapy with systemic chemotherapeutics or checkpoint inhibitors might further optimize intraperitoneal virotherapy protocols [120, 121].

1.3 Pressurized IntraPeritoneal Aerosol Chemotherapy (PIPAC)

An inhomogeneous drug distribution limits the efficacy of available, liquid-based intraperitoneal drug delivery methods. Moreover, the high intratumoral pressure restricts drug penetration into the tumor, resulting in low drug uptake in the target tissue and limited therapeutic efficacy [122].

Pressurized IntraPeritoneal Aerosol Chemotherapy (PIPAC) is a new drug delivery technique overcoming the limitations above [123]. During PIPAC, cytostatics are applied into the abdominal cavity as an aerosol under pressure. This artificial pressure counteracts the high intratumoral pressure to increase the drug uptake into the target tissue [124, 125]. PIPAC's superior pharmacological properties allowed a chemotherapeutics dose reduction by 90% [124, 126].

PIPAC also improves the homogeneity of drug distribution, as compared to a liquid solution. In contrast to liquids (which have a volume but no shape), a gas has no volume and no shape. An aerosol is a two-phase physical state comprising gas and suspended liquid droplets [127]. Thus, as compared to liquids, the physical properties of aerosols contribute to a more homogeneous spatial distribution

throughout the abdominal cavity [124, 125, 128, 129]. However, since aerosols sediment due to gravity, homogeneity remains imperfect and varies over time.

PIPAC is a minimally-invasive procedure that can be repeated several times, allowing repeated staging and objective assessment of tumor response [130, 131]. For example, a phase-II clinical study in patients with PM from gastric cancer achieved a histological tumor response in 60% of cases with a median survival of thirteen months, which is encouraging. This lower dosage of chemotherapeutics contributed to a lower plasma concentration, reduced systemic toxicity, and essentially prevented typical side effects of cytotoxic drugs [125].

1.3.1 Principle of PIPAC

PIPAC takes advantage of the closed, expanded abdomen to deliver drugs into the abdomen during a staging laparoscopy [123, 132]. The current technology aerosolizes droplets at high speed into carbon dioxide without a gas flow. These droplets possess high kinetic energy, and the primary mechanism of deposition is impaction. Since the aerosol particles are subject to gravitation, they also sediment over time.[133]. Brownian motion of suspended particles is observed, defined as the continuous interaction or colliding of suspended aerosol particles with each other and with the borders of the space in which they move. During PIPAC, aerosol particles create continuous pressure on the exposed peritoneum [134]. An extensive set of experimental data supports the benefit of increasing intraperitoneal hydrostatic

pressure for increasing tissue drug uptake [135-137]. This artificial hydrostatic pressure exceeds the interstitial fluid pressure, which is elevated in tumor nodes [138]. Along with this pressure gradient, the macromolecular drugs are dragged (by convection) from the peritoneal cavity into the tumor nodes and the normal subperitoneal tissue [139]. Since elevated intraperitoneal pressure also reduces portal and venous outflow [140], the systemic drug clearance is reduced during PIPAC application time. As a result, PIPAC enhances local tissue drug absorption [129], improves the spatial homogeneity of drug distribution [123] and reduces systemic exposition vs. available comparators.

Technically, the therapeutic aerosol is generated by a pressure-driven, mechanical medical device (CapnoPen®, Capnomed

GmbH Zimmern o.R., Germany) analogous to a common-rail diesel engine injector (Figure 3), [123, 141]. An upstream pressure of 11-20 bar is applied on the therapeutic solution using an angio-injector (Accutron HP-Thera®, Medtron AG, Saarbrücken, Germany) [123]. The pressurized solution drives the nebulizer by inducing rotation of a cylinder, and the shear forces micronize the liquid into tiny aerosol droplets. The intraabdominal pressure (12-15 mmHg) is generated by a conventional CO_2-insufflator (e.g. Thermoflator®, Karl Storz GmbH, Tuttlingen, Germany) and is not modified by the aerosolization process. In contrast to most aerosol generation technologies, there is no gas flow needed for aerosolizing the chemotherapy solution. The tightness of the system is essential for occupational health safety reasons. Since there is no gas exiting, all the drug aerosolized

remains within the abdomen, allowing precise determination of the drug dose applied. The distribution of droplet sizes is bimodal, with the first peak at 3 um (fine fraction) and the second peak at 37 µm (coarse fraction). The overwhelming part of the liquid (volume%) was aerosolized as larger droplets, droplets with a diameter of 3 um (fine fraction) representing only 2.5 vol%. However, the Capnopen® generates a considerable particle cloud. More than 92.5 number% of the released droplets have a diameter above 3 µm. Notably, the droplets' size does not vary between aqueous and lipidic test solutions, so that the device can be considered polyvalent.

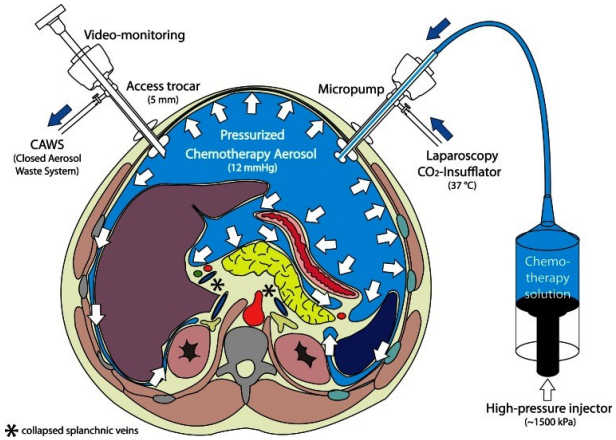

***Figure 3*: PIPAC: technical components**

The normothermic CO_2-pneumoperitoneum is installed using an industry-standard CO_2- insufflator. Then, a dedicated aerosolizes is inserted into the abdomen through an access trocar, The aerosolizer is connected to a chemotherapy syringe via a high-pressure line. The syringe is placed into an industry-standard high-pressure (angio-)injector. The chemotherapy solution is aerosolized into the abdomen and the system is kept in steady-state for 30 min application time. Then, the toxic aerosol is exhausted safely over a Closed Aerosol Waste System (CAWS) into an appropriate filter. Reproduced with permission from [132].

However, based on our data in ex vivo, the most significant tissue penetration depth was revealed in the tissue opposite to the nozzle,

which is easily explained by the impaction forces of the aerosol droplets. Thus, the position of the nozzle influences tissue drug penetration and concentration.

1.3.2 The PIPAC procedure

The PIPAC procedure has been described in detail elsewhere [124]. Shortly, PIPAC is a laparoscopic procedure performed under general anaesthesia. After insufflation of the CO_2-pneumoperitoneum, two trocars are placed through the abdominal wall to permit access to be abdomen. First, the surgeon removes the ascites, if any. After the introduction of a video camera, he quantifies the extent of peritoneal spreading using the Peritoneal Cancer Index (PCI) [142]. Multiple tissue biopsies in all four quadrants are taken to determine histologically the tumor's regression grade using the Peritoneal Regression Grading

Score (PRGS) [69]. Adhesiolysis is not performed routinely.

Then, the chemotherapy syringe is placed into the angio-injector. The CapnoPen® is inserted into a trocar and connected to the high-pressure injector. The tightness of the abdomen is controlled. The team leaves the operating room; the following steps are remote-controlled to ensure personal safety [143]. The chemotherapy solution is aerosolized at a flow of 0.5-0.7 ml/sec and maintained in steady-state for an exposure time of 30 min. The toxic aerosol is exhausted safely into the external environment over a closed aerosol waste system (CAWS). All inserted trocars are removed upon completing the procedure, and the wounds are sutured [124].

1.3.3 The need for further optimization of PIPAC

Since 2011, PIPAC has been used in over 12.500 applications in human patients worldwide. Whereas PIPAC technology has been shown to be safe and effective, the procedure is still in its infancy, and the space for improvement is significant. PIPAC is not a therapy but a drug delivery system improving the target effect of a given drug. This goal can be achieved:

- by dedicated drug formulations (e.g. lipophilic coating, delayed-release, etc.),
- by next-generation medical devices (better distribution), by environmental control within the abdominal cavity (e.g. hyperthermia or electrostatic loading),
- by changing the environment (e.g. by charging the aerosol with positive or

negative charge, increasing the temperature) and

- by combining these factors.

The system's complexity necessitates a so-called "quality-by-design" approach, where key quality attributes of the different system components are determined depending on their expected effect on the target tissue. This backward approach is common in pharmaceutical development [144] and applies perfectly to the peritoneum as a novel field of research.

1.4 Preclinical models for PIPAC optimization

Whereas some aspects of PIPAC research can be simulated in-silico [145], numerous experiments are needed before technological or pharmaceutical advances can be translated into clinical practice. Several *in vitro*, *ex vivo*,

and *in vivo* models have been described allowing the investigation of the effects of a therapeutic aerosol on the peritoneum.

1.4.1 In vitro cell culture models

In vitro cell culture models are routinely used for functional assays in cancer research. A PubMed query with the keywords "cell lines" and "HIPEC" on Nov 23rd, 2020 retrieved 3529 articles. For example, our group examined the chemosensitivity of various peritoneal cancer cell lines to HIPEC and PIPAC [146]. Reviewing this abundant literature would go well beyond the focus of the present work.

After restriction to three-dimensional models, only 11 studies were retrieved. These studies were published recently, showing a growing interest in *in vitro* models beyond traditional cell culture. For example, a three-dimensional model of the human mesothelium was

established to investigate early metastasis steps in ovarian cancer [27]. This model used two layers, a deeper layer containing fibroblast mixed with collagen I and a superficial layer consisting of mesothelial cells. After the mesothelial layer achieved confluency, SKOV3 human ovarian cancer cells were seeded on the top. This model allowed histological analysis and functional adhesion assays.

Our group has recently developed an organotypic 3D model of the human peritoneum. Using this model, we could measure the adhesion and the invasion of MKN45 gastric cancer cells (Castagna A et al., unpublished data).

1.4.2 Ex vivo models

1.4.2.1 Hermetic plastic box

The first *ex vivo* model to evaluate drug distribution and tissue penetration after PIPAC

was a 3-4 L hermetic plastic box containing tissue fragments placed at different locations (Figure 4), [129]. This model was used for evaluating the distribution, and the immediate biological effect of siDNA applied as PIPAC on normal and diseased peritoneal tissue immediately after surgery. Further studies used the hermetic plastic box to evaluate:

- the homogeneity of spatial distribution after PIPAC [147],
- the influence of the position of the CapnoPen® position,
- the role of drug concentration, and
- the effect of increasing CO_2 pressure [148] and hyperthermia (unpublished data).

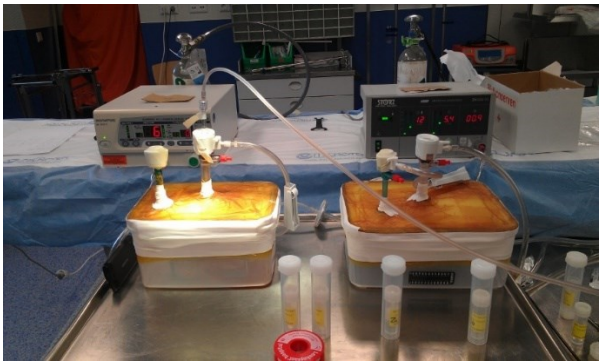

***Figure 4*: Ex vivo model: Hermetic plastic box.** *Here an experiment evaluating the effect of hyperthermia on tissue drug uptake, using a normothermic (left) vs. hyperthermic (right) CO2-insufflator. Picture: courtesy of Prof. M.A. Reymond.*

1.4.2.2 Inverted bovine urinary bladder (IBUB)

The *ex vivo* plastic box has several limitations. Most importantly, the plastic walls do not absorb any liquid; there is aerosol condensation on the plastic walls and all the liquid collects on the bottom of the model. In 2017, our group established an innovative *ex vivo* model for optimizing therapeutic aerosols: the inverted bovine urinary bladder (IBUB) (Figure 5). The

idea was elegant: anatomically, the bovine bladder is almost completely covered with peritoneum, which becomes the organ's internal lining when it is inverted (outside-in). The IBUB creates an organic structure lined with peritoneum with a volume similar to the human abdomen (2-4 L). The IBUB model allows morphological, pharmacological, and short-term biological analyses. A significant aspect of the IBUB is that it does not require animal sacrifice [149].

Technically, fresh bovine urinary bladders from the slaughterhouse are stored under 2-4°C and immediately delivered to the lab, where the organ is rinsed with water, and surrounding fat tissue is excised. The organ is inverted, a 12-mm balloon trocar is placed through the bladder neck and fixed with a suture. Next, CO_2 is insufflated into the inverted bladder up to 12 mmHg, a nebulizer is inserted into the trocar,

and a therapeutic solution is aerosolized under selected environmental conditions. Each parameter can be modified independently.

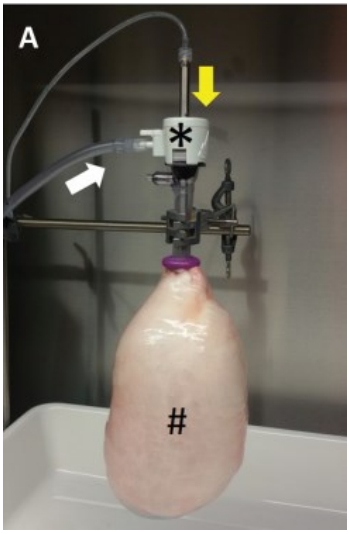

***Figure 5*: the Inverted Bovine Urinary Bladder (IBUB) model.**
*A fresh urinary bladder from, the slaughterhouse is inverted (outside-in) so that the inner surface of the organ is lined with mesothelium, with a volume similar to the expanded human abdomen. # - IBUB, * - balloon trocar, A – high-pressure line. Arrow: position and direction of the aerosolizer (Capnopen®) [149].*

1.4.3 Animal models

According to the "3R" principles (Replacement, Reduction, Refinement), modern biomedical research needs to reduce experiments in living animals to a minimum [1]. However, animal experiments remain necessary for confirmatory preclinical studies. Moreover, Institutional Review Boards and regulatory authorities usually require toxicity studies in two animal species before first-in-human use.

1.4.3.1 Mice model

There is a single study in the mouse evaluating the pharmacokinetics of chemotherapy delivery by PIPAC [150]. Due to the animal's small size, it was impossible to use the Capnopen® device, and the authors generated the therapeutic aerosol using the millimeter-sized

1 We are contributing to the „3R Center Tübingen für In-vitro-Modelle und Tierversuchs-alternativen“, www.3rtuebingen.de .

pipe of an HPLC device. This study delivered valuable results on the comparative pharmacokinetics of PIPAC vs. HIPEC in the mouse. However, the protocol used low pressure, small volumes, minimal drug dosage, and another medical device, so extrapolation of results to the human must remain careful.

1.4.3.2 Rat model

Recently, an *in vivo* PIPAC model was established in the rat. Wistar rats' body weight is around 300 g, about ten times larger than mice. For the experiment, special Capnopen® devices with a diameter of 5 mm were engineered by the manufacturer. The operating setup included intrabdominal placement of two trocars with eight mmHg intraabdominal pressure. All animals survived the procedures with no deterioration in general condition. Repeated PIPAC under general anaesthesia was possible with an interval of three weeks.

Thus, the rat model is feasible and safe for intraabdominal aerosol studies [151]. With at least 156 publications [152], multiple models of PM have been established in the rat, allowing not only pharmaceutical / toxicity but also efficacy studies in several cancer types.

1.4.3.3 Rabbit model

To our knowledge, there is a single rabbit model of PM [153], established with transfected human uterine squamous cancer cell lines (VX2) [154]. The authors used this model for a pharmacological distribution study of nano-formulated paclitaxel delivered as HIPEC [155], not PIPAC. The rabbit model has the advantage of more significant animal weight (between 2-6 kg, representing ten times the weight of a rat and 100 times a mouse's weight). However, to our knowledge, there is only a single cell line used to generate PM in the rabbit, and this cell line has uncommon histology for PM.

1.4.3.4 Swine model

Minipigs in the laboratory have a bodyweight of around 30 kg. An advantage of the minipigs as a model for optimizing intraperitoneal drug delivery is their comparable size and weight with the human being. Identical parameters as in the human (drug dosage, formulations, medical devices, intraabdominal pressure, etc.) can be used. Moreover, the pig has an immune system mainly similar to the human [156]. Thus, results obtained with PIPAC in the swine can be better extrapolated to the clinical situation than results in rodents.

Swines were widely used for PIPAC research. For example, the superiority of spatial distribution of methylene blue delivered as PIPAC was superior vs. normothermic intraperitoneal lavage was first shown in German landrace pigs [123]. Several pharmacokinetic / pharmacodynamic studies

compared PIPAC vs. HIPEC [157] and PIPAC vs. ePIPAC [158] in the swine. Our group has established a pig model of surgical tumor recurrence in peritoneal wounds [159], but an allograft or xenograft model of PM has not been reported so far. To our knowledge, pigs do not develop PM, and there is no spontaneous model of peritoneal cancer in this species.

1.4.4 Limitations of current models

All pre-clinical models above show limitations for peritoneal research. The *in vitro* two-dimensional cell culture models using commercial human mesothelial and fibroblast cell lines are easy to use and versatile. Such cell lines allow chemoresistance studies, gene expression comparisons, and functional experiments. However, two-dimensional cell lines cannot reproduce the complex anatomy and composition of the peritoneum and the subperitoneal tissue. Moreover, a clonal

selection is observed after multiple passages. Thus, it is not easy to extrapolate the results to the situation in-vivo. Using primary peritoneal cell lines derived from samples collected in the operating room limitation can circumvent, in part, this limitation.

The three-dimensional organotypic human peritoneal model is a further step in developing alternatives to animal experiments. Asano established a three-dimensional organotypic human peritoneal model similar to *in vivo*-derived tissue. This model reproduces the peritoneal morphology and metabolic processes well and is considered the best in-vitro model available. However, it remains an approximation since the tissue generated does not reproduce the *in-vivo* complexity due to the lack of mediators, hormones, vasculature, nerves, interaction with other cells, etc. [160]. Furthermore, the three-dimensional cell culture

model is millimetric, and it is impossible to engineer a whole organ resembling the abdominal cavity.

The *ex vivo* model placing tissue samples inside a plastic box allows experiments on freshly prepared human tissue, a significant advantage over the *in-vitro* models described above. However, the tissue is not vascularized anymore and is thus highly hypoxic. Therefore, tumor metabolism is modified, and only short-term experiments over a few hours are meaningful. Moreover, most of the box surface is not covered with serosa [148], and aerosol condensation on the plastic walls leads to liquid collection on the bottom.

Schnelle et al. proposed with the IBUB (see above) another original and attractive *ex vivo* model [149]. The IBUB model is a full-size model of the abdominal cavity. Its inner aspect

is lined by serosa. The IBUB model allows standard PIPAC technology and parameters such as pressure, temperature, charge, etc. However, the IBUB model does not allow measurement over time so that dynamic measurements require the multiplication of experiments.

Animal models are the most sophisticated models for peritoneal research. However, as summarized in Table 1, there is no ideal animal choice for modelizing PIPAC. Most models available are too small for realistic experiments. There is no PM (spontaneous or xenograft) model in the swine or the sheep, the only full-size animals available for experimental PIPAC research.

***Table 1*: Different research questions – different animal models.**

Animal	Weight	Healthy model	PM model	PIPAC Instruments	Pressure
Mouse [150]	0.03 kg	Yes	Yes	N/A	No
Rat [151, 161-164]	0.3 kg	Yes	Yes	5 mm	6-8 mmHg
Rabbit	3 kg	Yes	Yes	5mm	6-8 mmHg
Sheep [165]	30 kg	Yes	No	Standard (9 mm)	12-15 mmHg
Swine [123, 125, 158, 166-174]	≥70 kg	Yes	No	Standard (9 mm)	12-15 mmHg

A further challenge is the regulatory barriers for performing experiments in living animals. Modern biomedical research is required to replace animal experiments with alternative models, reduce the number of animals involved, and refine the experiments to minimize the animals' burden. Animal models are expensive, require dedicated facilities allowing proper care and medication [151, 155, 175]. Further limitations of animal models are the peritoneal cavity's complex anatomy,

complicating spatial drug distribution interpretation. Drug uptake into the parietal vs. visceral peritoneum is radically different [158]. Finally, experiments over time are difficult or impossible to perform, so that dynamic measurements in real-time would require many animals. As a result, it is challenging to investigate aerosol's effects on target tissue in animal models. In the absence of specialized knowledge, a direct comparison between samples can lead to data misinterpretation.

1.5 Knowledge gap

Despite the variety of approaches available, no peritoneal model allows real-time measurements of tissue drug absorption. No model enables us to differentiate between the direct, immediate effect of the aerosol on drug uptake and the indirect, sustained impact of the liquid sedimenting to the bottom of the peritoneal cavity.

1.6 Research objectives

The main objective of this study is to develop a new peritoneal model *ex vivo* allowing:

- Repeated pharmacological measurements over time,
- Determination of the effect of the aerosol vs. the liquid sedimenting.

The hypothesis was that the following measurements are possible in the new model:

- Determining tissue aerosol absorption over time,
- Calculating aerosol sedimentation over time,
- Assessing tissue drug uptake by the aerosol alone (drug concentration),
- Measuring the depth of tissue drug penetration by the aerosol alone.

2 Materials and Methods

2.1 Study design

This is an *ex vivo* study in explanted animal organs. The state-of-the-art Inverted Bovine Urinary Bladder (IBUB) model proposed by Schnelle provided the basis for the current study [149]. In a first step, a list of specifications for an enhanced *ex vivo* model allowing real-time measurements of liquid and drug uptake into the peritoneal tissue was defined. In a second step, the technical modalities were set up and the enhanced IBUB (eIBUB) model established. In a third step, the eIBUB model was validated by comparing its performance with the original IBUB model.

2.2 Regulatory framework

This research did not involve human sample or living animals. No animal was sacrificed for this study. According to German law, no

authorization of the Ethics committee or the Animal Research Committee was required.
All experiments were performed at the laboratories of the National Center for Pleura and Peritoneum, University of Tübingen, Germany, between June 2017 and November 2020.

2.3 Study groups, sample size

In the validation step of this study, pharmacological results obtained in the enhanced IBUB model (eIBUB) were compared with results obtained in the original IBUB model (Figure 6). Our hypothesis was that no difference would be observed in:

- Depth of tissue penetration of doxorubicin,
- Tissue concentration of cisplatin and doxorubicin,

- Homogeneity of spatial distribution of cisplatin and doxorubicin.

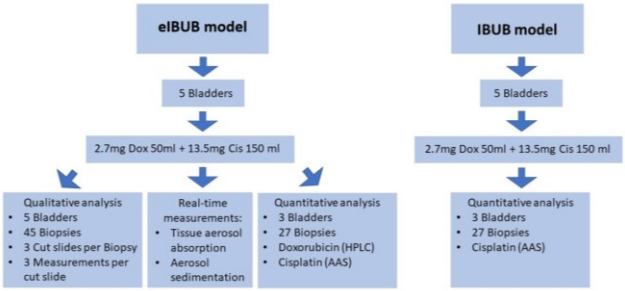

Figure 6: Study groups comparing the eIBUB vs. IBUB models.
Three groups were created for qualitative, quantitative, and real-time pharmacological analysis in the eIBUB model (left panel). The results were compared with the available IBUB model (right panel).

All experiments were performed in triplicate with three biopsies at three levels in three different organs, resulting in 27 samples per group analyzed. Real-time measurements of liquid tissue uptake and aerosol sedimentation were only possible in the enhanced IBUB (eIBUB) model.

2.4 Organ procurement and preparation

In the early morning of the experiments' day, bovine urinary bladders were explanted in the slaughterhouse and delivered directly to the NCPP laboratory. For each experiment, three fresh bladders with a weight of 120-190 g and a length of 12-15 cm were selected. Any damaged organ was excluded. The organs were rinsed with water, dried with a paper towel, and covered with a humid drape. The perivesical fatty tissue was excised, and the organ inverted through the bladder neck (outside-in) using forceps. A 12 mm double-balloon trocar (Kii, Applied Medical, Düsseldorf) was inserted into the bladder neck and secured with a running suture to ensure tightness. The inner balloon was inflated. The trocar was connected via plastic tubing to a CO_2 insufflator (Endoflator®, Karl Storz GmbH, Tuttlingen,

Germany). The IBUB was placed into the working bench and hanged up using a laboratory tripod at 60 cm height. A flat container was positioned under the organ for collecting liquid dripping down.

2.5 Chemotherapeutic drugs and solutions

The chemotherapy syringes were prepared ahead of the experiment. The drugs doxorubicin (DOX) and cisplatin (CIS) were selected because they are the most used during PIPAC [176]. Moreover, doxorubicin is particularly interesting since:

- DOX tissue penetration is minimal (10-30 µm).
- DOX has a spontaneous fluorescence at 560 nm enabling direct assessment of tissue penetration with fluorescence microscopy.

Following drug solutions were prepared:

- Doxorubicin hydrochloride, 2.7 mg (Cell Pharm® GmbH, Bad Vilbel, Germany), dissolved in 50 ml NaCl 0.9%,
- Cisplatin, 13.5 mg (Teva® GmbH, Ulm, Germany) dissolved in 150 ml NaCl 0.9%.

The drugs were homogenized with a magnetic stirrer (S1 Basic Magnetic Stirrer, Fisher Scientific GmbH, Schwerte, Germany) and pipetted into separate 200 ml high-pressure syringes (Nr. 316026-000, Medtron AG, Saarbrücken, Germany).

2.6 Application of chemotherapy

The chemotherapy syringes were placed into the head of a high-pressure angio-injector (Accutron HP-Thera®, Medtron, Saarbrücken,

Germany) at room temperature. An aerosolizing device (Capnopen®, Capnomed, Zimmern o.R., Germany) was inserted into the trocar and connected with the syringes via a high-pressure line. Drugs were aerosolized into the IBUB at a flow between 0.5 and 0.7 ml/sec depending on the conditions. The system was kept in steady-state for 30 min. Then, the toxic aerosol was released over a Closed Aerosol Waste System (CAWS) into HEPA filters.

2.7 Sampling and pre-analytical sample processing

After complete aerosol release, the bladder was opened longitudinally under a safety hood. Nine transmural punch biopsies with a diameter of 8 mm were taken at the top, at the middle and at the bottom of the IBUB, totalizing 27 biopsies/bladder. Biopsies were placed in 12-well sterile plastic plates and immediately frozen at -80º C.

For measurements of the depth of tissue penetration, samples were fixed with Tissue-Tek (Sakura REF 4583, Umkirch, Germany) and cut into 10 µm thick sections using a cryotome (Leica CM3050S, Jena, Germany). From each biopsy three sections were taken. Sections were air-dried at RT.

For drug concentration measurements, samples were lyophilized (Speedevac KF-2-110; H. Saur Laborbedarf, Reutlingen, Germany) and weighed allowing normalization to "dry weight". The pellets were cut into small pieces and resuspended into 1 ml distilled water. Then, samples were homogenized using high-energy ceramic beads in an automatized device (micro-D9, MICCRA GmbH, Heitersheim, Germany) for 1 min. Then, samples were sonicated (Elmasonic S10, Elma Schmidbauer GmbH, Singen, Germany) for 20 min and placed in an overhead rotator overnight

(Roto-Mix, neoLab, Heidelberg, Germany). Samples were diluted with 0.5 ml distilled water to a final volume of 1.5 ml. After vortexing and centrifugation, samples were stored at -80°C until shipping.

2.8 Analysis of depth of tissue penetration

Qualitative analysis of doxorubicin tissue penetration was performed by fluorescence microscopy (Quantimed Q 600, Leica, Germany). Three sections were taken for each biopsy, and measurement of each section was performed in triplicate. Analysis was performed by a pathologist or by a technical personal trained by a pathologist. Microscopic examination was blinded to the origin of the sample. First, the general condition of the sample was documented by taking an overview picture (magnitude 2.5x). Next, the presence of fluorescence in the tissue at an emission

wavelength of 490 nm and an absorption wavelength of 560-590 nm, and the distance from the surface was determined (Qwin software 2002, Leica). The software and the microscope were standardized using a standardizing scale bar before measuring.

2.9 Analysis of drug tissue concentration

Quantitative analysis of doxorubicin and cisplatin was performed by an examined chemist in an external, GLP-certified laboratory (Medizinisches Versorgungszentrum Dr. Eberhard & Partner, Dortmund, Germany). Cisplatin was quantified by atomic absorption spectroscopy (AAS; ZEEnit P 650, Analytic Jena AG, Jena, Germany). The lower level of quantification (LLoQ) for platinum was 50 ng/ml (cisplatin 80 ng/ml; calculation factor 1.54). Preanalytical validation proved a linear range of measurements in 5% glucose matrix between

0.1 and 100 µg/ml platinum and established no influence of organic matrices. Doxorubicin was measured by high-performance liquid chromatography (HPLC, Waters Fluorescence Detector 2475, Waters Inc., Milford, MA, USA), with a serum LLoQ of 5 ng/ml. Preanalytical validation proved a linear range of measurements in 5% glucose matrix between 0.1 and 10000 µg/ml doxorubicin and established no influence of organic matrices.

2.10 Occupational health safety

The experiments described in this study are potentially harmful to the persons involved and should not be performed without proper equipment and qualification. Toxic aerosols with cisplatin and doxorubicin were manipulated during this research. NCPP research labs are equipped for using harmful aerosols, and the persons involved are trained. All experiments were performed under a high-

performance safety working bench (Maxisafe 2020, Thermo Electron LED GmbH, Langenselbold, Germany) equipped with HEPA filters allowing safe manipulation of cytotoxic drugs. Bladders were prepared under a mobile HEPA air filtering unit. NCPP labs were the object of an independent safety audit in fall 2016, the lab is regularly cleaned, and surface probes are taken to detect possible contamination with platin traces.

2.11 Statistics

Data were entered into Excel tables (Microsoft Office, Microsoft Corp., Washington, USA). Descriptive statistics include mean and 95% CI. The H0-hypothesis was that there is no difference in the above parameters between the eIBUB and IBUB models. Since most data were not normally distributed, comparisons between groups were performed using non-parametric tests, typically Mann-Withey test or ANOVA.

For statistical analysis, we used SPSS software package v. 25 (IBM, NY, USA).

3 Results

3.1 Requirements and specifications for a new ex-vivo peritoneal model

In the introduction, we have analyzed available models, identified the knowledge gap and shown the need for a new peritoneal model. The purpose of this work was to develop a new peritoneal ex vivo model superior to available comparators that meets the following expectations:

- Repeated pharmacological measurements over time,
- Determination of the tissue effect of the aerosol vs. the liquid sedimenting.

For prioritizing the development work, designing and validating the new model, we used the following requirements list (users' expectations: what the model shall provide) and

specifications (development team's assumptions):

***Table 2*: Requirements list and specifications for the elBUB model.**

Requirements	
Functional requirements	measurement of the tissue drug concentration
	measurement of the depth of drug tissue penetration
	assessment of the homogeneity of spatial drug distribution
	measurement of tissue liquid uptake in real-time
	measurement of the aerosol sedimentation in real-time
Usability requirements	PIPAC and ePIPAC are feasible in the model
	can be easily setup and can be used by a trained laboratory technician
Ethical / regulatory requirement	no use of living animals
Financial requirements	material costs below 100 € / experiment

Specifications	
Non-functional specifications Technical specifications	steering of intraluminal parameters (pressure, temperature, pH, etc.)
	monitoring of these parameters, including video monitoring
	taking biopsies
	is covered by peritoneum
	creates a tight space
	has a volume of 3-5 liters
	can be expanded with a gas
	tolerates an intraluminal pressure of up to 20 mmHg
	collects the aerosol sedimenting / the liquid dripping down along the walls
	offers a digital interface for real-time data collection
Environmental specifications	can be used within a safety laboratory hood
	has a closed aerosol waste system (CAWS)
Interaction specifications	drugs can be applied as a liquid, gel, powder

	can accommodate various aerosolizing devices

3.2 Design of the enhanced IBUB model (eIBUB)

The eIBUB model builds upon the IBUB and adds significant features. The eIBUB model's principle is illustrated in Figure 7. The central component of the eIBUB, as the IBUB, is an inverted bovine urinary bladder. The inverted bovine bladder modelizes the human peritoneal cavity. The bladder is connected to an industry-standard CO_2-insufflator expanding the organ at a pressure of 12-15 mmHg. A trocar is inserted through the bladder neck and secured via a pursuing suture, preventing any gas or aerosol leakage [177].

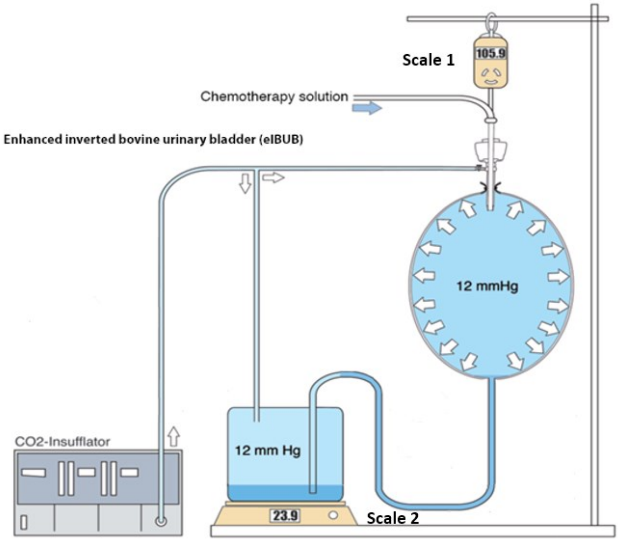

***Figure 7*: Principle of the enhanced IBUB model ("eIBUB").**
System components are a CO_2-insufflator, the inverted bovine bladder, a second vessel connected to the bottom of the bladder, and two scales measuring in real-time the weight of the bladder and the vessel.

The expanded eIBUB has a volume similar to the expanded human abdomen (3-5 L). The inner lining consists of serosa (the parietal peritoneum, which has been turned outside-in) [177].

As compared to the previous art (IBUB model), two significant innovations have been introduced into the eIBUB's design:

3.2.1 Communicating vessels principle

The eIBUB is connected to a second vessel, taking advantage of the communicating vessel principle (Figure 8) [177]: the fluid level of two communicating vessels will remain at the same level in the vertical plane, assuming both vessels are kept at the same pressure. This, when setting the level of the second vessel slightly below the bottom of the bladder, the liquid falling along the bladder lining is continuously collected and evacuated into the second vessel. This allows to monitor in real-time the aerosol sedimentation.

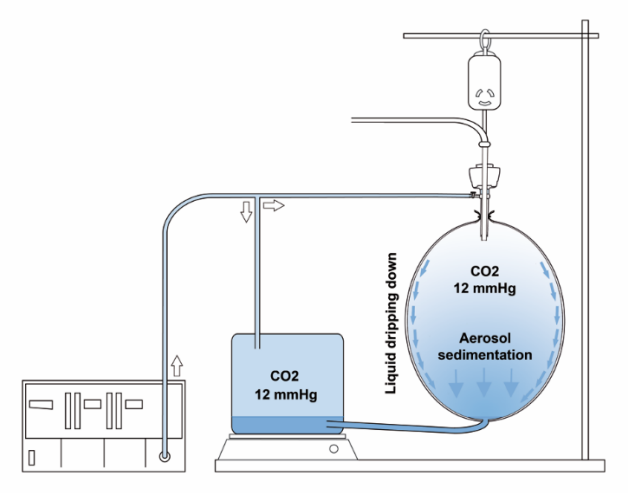

***Figure 8*: eIBUB model: Principle of the communicating vessels.**
Application of the principle of the communicating vessels in the eIBUB model. Both vessels are connected vis a tubing stitched at the base of the organ. The intraluminal pressure is kept continuously the same in both vessels.

Schematically, a silicone tubing is sutured at the base of the organ and connected to an airtight plastic container of a sufficient volume (Figure 8) [177]. The tubing is first filled with water (siphon) to prevent aerosol from escaping from the IBUB and flowing to the second vessel. This second vessel is connected via a second

Y-tubing to the CO_2-insufflator, which maintains an identical pressure at every point of time.

The technical setup of the connection and the second vessel is illustrated in Figure 9. Two 16-mm holes are drilled in the cap and the side industry-standard, 200 ml hermetic plastic bottle (Kautex Textron, Bonn-Holzlar, Germany).

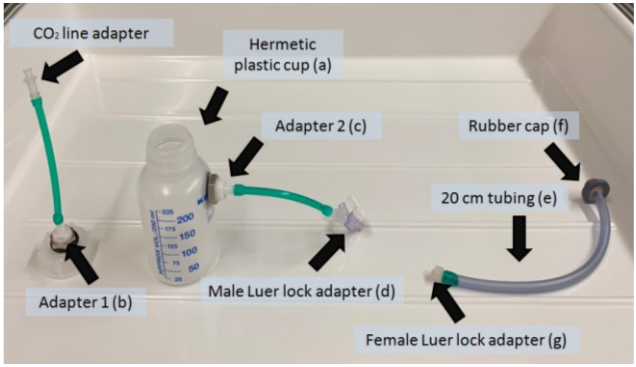

***Figure 9*: Technical details of the second, communicating vessel.**
The CO_2-line from the insufflator is connected to the top of the bottle via an adapter (b). A second adapter (c) is tightened to the side of the bottle and connected with a male Luer-lock (d). After perforating the bottom of the IBUB, a rubber cap (f) is placed and tightened with a pursuing suture. The IBUB is connected to the hermetic

plastic cup via a 20 cm long, 5 mm diameter silicone tube (e) via Luer lock adapters (d) and (g).

3.2.2 Real-time weight monitoring

The bladder and the second vessel are weighted independently in order to be able to measure the bladder weight gain over time as well as the weight of the liquid sedimenting over time (Figure 10) [177].

- Bladder weight (Weight 1):

  The bladder is hanging to a scale or, alternatively, the bladder and its tripod are placed on a scale. The initial weight is determined (tripod, trocar, lining, and the bladder weight at the beginning of the experiment). Any change in the measured weight reflects a shift in the bladder's weight. The weight shift is not due to the liquid (since the falling fluid is continuously collected at the basis of the organ). Thus, the first balance provides a real-time value

of the aerosol uptake into the tissue. For optimizing aerosol delivery, this value has to be maximized.

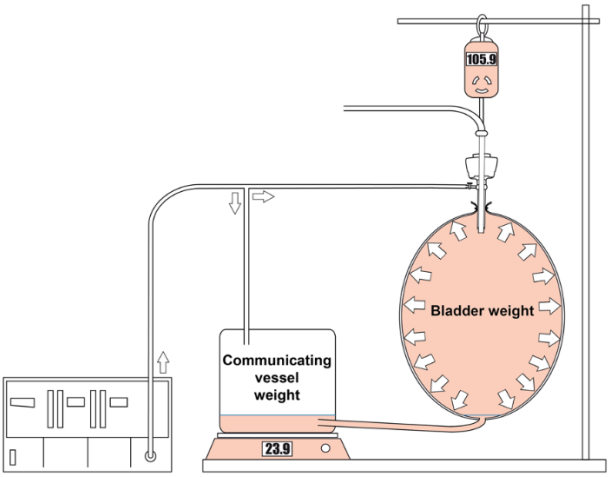

Figure 10: ***Principle of the independent weighting.*** *The weight of the bladder and the communicating vessels are weighted independently, allowing a real-time measurement of the aerosol tissue uptake and of the liquid falling to the base of the target organ.*

- Weight of the communicating vessel (Weight 2)

The communicating vessel is placed on a second scale. The total volume of the

aerosol sedimenting and the liquid dripping down the inside bladder wall is immediately collected into the communicating vessel. Thus, the second balance provides a real-time value of the aerosol not reaching the target tissue. Alternatively, it is possible to measure not the weight but the liquid volume in the communicating vessel. For optimizing aerosol delivery, this value has to be minimized.

Since the drug concentration in the aerosolized solution is known, the combination of weights 1 and 2 provides accurate real-time data on the volume of drug solution taken up into the tissue.

3.3 Implementation of the eIBUB in the research lab

The experimental bench is illustrated in Figure 11. The whole eIBUB system was placed in a

safety hood allowing safe manipulation of toxic aerosols. The inverted bladder can be easily recognized in the centre. The bottom of the bladder was connected to a hermetic vessel (a) placed on a balance (b) (PCB 600-2, Kern GmbH, Balingen, Germany).

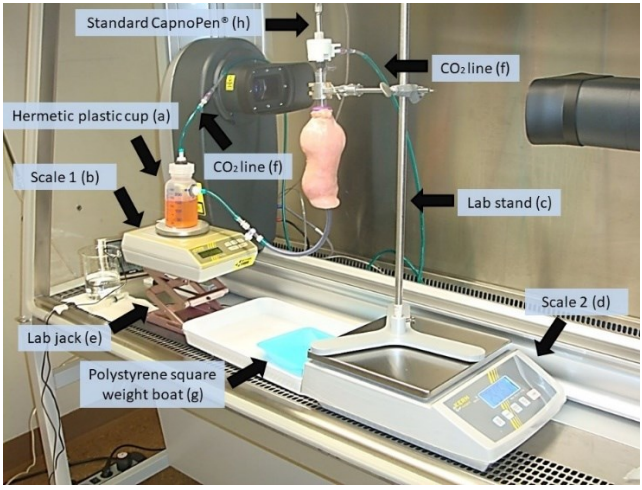

***Figure 11*: elBUB model: experimental bench.**

The IBUB itself is hanging in a tripod (c) placed on a balance (d) (FCB12K1, Kern GmbH, Balingen, Germany). The vertical position of the

second vessel was adjusted precisely to the level of the bottom of the bladder. CO_2 was supplied by an industry-standard laparoscopy insufflator (Endoflator®, Karl Storz GmbH, Tuttlingen, Germany). The bladder and the communicating vessel were insufflated over a branched silicone line (f) to ensure equal CO_2 pressure in both volumes. The aerosolizer (h) (Capnopen®, Capnomed, Zimmern, Germany) was inserted into the bladder. A polystyrene recipient (g) was positioned between the two scales to collect any liquid transudation through the bladder wall during aerosol application. Weight data are captured from the digital output to the balance (lab jack, e), transferred via VGA connection to a laboratory software (Kern® Balance Connection, Kern SCD 4.0, Kern and Sohn Ltd., Balingen, Germany) running on an industry-standard laptop computer (ASUS, F515EA-BQ477, ASUS, Taipeh, Taiwan).

3.4 Verification of the eIBUB model

Verifying the eIBUB model focuses on its analytical performance to answer whether the model has been developed correctly. This confirmation requires examination and provision of objective evidence that the specified requirements are fulfilled and specifications have been appropriately chosen.

The main results of the verification of the eIBUB model are summarized in the following Table.

Table 3: Verification of the requirements of the eIBUB model.

Requirements		**Verification**	
Functional requirements	tissue drug concentration	Platin-based drugs	Yes
		Anthracyclins	Yes
		Taxanes	Yes
	depth of tissue drug penetration	Platin-based drugs	Not verified
		Anthracyclins	Yes
		Curcumin	Yes

	homogeneity of spatial drug distribution	Platin-based drugs	Yes
		Anthracyclins	Yes
	the homogeneity of spatial drug distribution	Platin-based drugs	Yes
		Anthracyclins	Yes
	tissue liquid uptake in real-time	Yes	
	aerosol sedimentation in real-time	Yes	
Financial requirements	material costs below 100 € / experiment	15 € / bladder	Yes
Usability requirements	can be easily setup	< 20 min	Yes
	can be used by a trained laboratory technician	Not verified	
Ethical / regulatory requirement	No use of living animals	Yes	

3.4.1 Functional requirements

Functional requirements were measurement of the tissue drug concentration, the depth of tissue drug penetration, the homogeneity of spatial drug distribution, the tissue liquid uptake

in real-time and the aerosol sedimentation in real-time.

3.4.1.1 Measurement of tissue drug concentration

Measurements of tissue drug concentration were performed for a platin drug (cisplatin) and an anthracycline (doxorubicin), two cytotoxic drugs commonly used during PIPAC.

- Doxorubicin

Figure 12 illustrates the median doxorubicin tissue concentration for the top, middle, and bottom of three eIBUBs, determined on 27 biopsies.

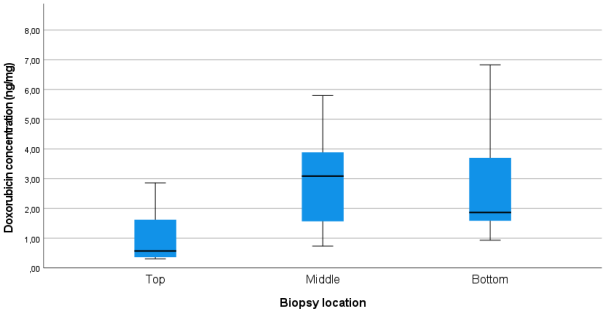

***Figure 12:* Doxorubicin tissue concentration at different positions in the eIBUB model.**

The highest concentration of doxorubicin (median: 3.09 ng drug/mg tissue) was seen in the middle part of the IBUBs. At the top, the median doxorubicin concentration was lower with a median of 0.57 ng/mg and higher at the bottom with 1.87 ng/mg. There was a relative difference of around 6x between the lowest and the highest concentration value. The difference in doxorubicin between the top and the middle (p=0.01), respectively, the middle and the bottom (p=0.03) were statistically significant. In contrast, the difference between the middle and the base did not reach significance. Thus,

doxorubicin distribution within the IBUB after PIPAC using the reference medical device was inhomogeneous.

- Cisplatin

Figure 13 illustrates the median cisplatin tissue concentration for the top, middle, and bottom of three eIBUBs, determined on 27 biopsies.

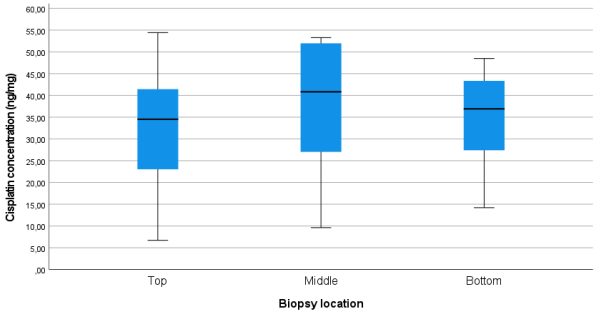

***Figure 13**: Cisplatin tissue concentration at different positions in the eIBUB model.*

Whereas the highest cispatin concentration (median 40.84 ng/mg) was observed in the middle of the bladders, the concentration difference was not significant between the various locations, with a maximum of 18%

between median values. Thus, cisplatin distribution in the eIBUB is more homogeneous than doxorubicin.

Since the same key quality attributes (device, pressure, exposition time, temperature) have been used in the experiments, tissue uptake also depends on the drug or its formulation.

3.4.1.2 Measurement of depth of drug tissue penetration

The depth of drug tissue penetration in the eIBUB model was determined by analyzing peritoneal biopsies taken at the end of every aerosolizing experiment. However, in theory, since trocars allow endoscopic access to the organ, such biopsies could also be taken in the eIBUB at various points of time over the course of the experimental procedure.

The analytic method to determine tissue penetration in the peritoneal biopsies depends on the drug used in the experiment. For

example, fluorescence microscopy was used to measure the depth of nuclear staining after aerosolization of doxorubicin, a cytotoxic drug (anthracycline) targeting DNA and creating double-strand mutations [178, 179]. Doxorubicin has a spontaneous fluorescence at an excitation wavelength of 470 nm and a capture wavelength of 560 nm [180]. Figure 14 shows a representative example of such a fluorescence microscopy measurement.

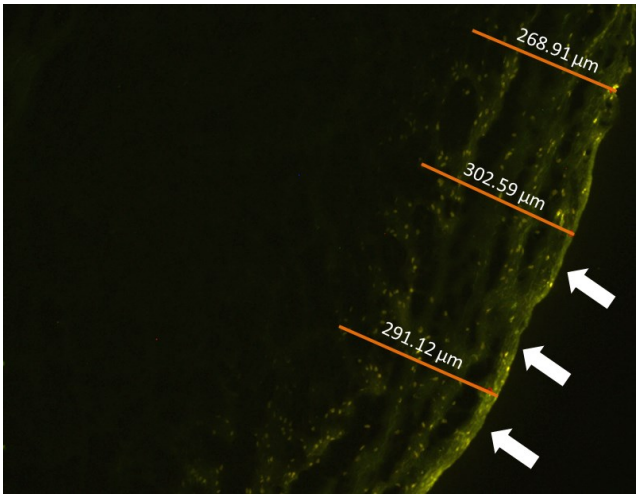

***Figure 14*: Depth of tissue doxorubicin penetration (fluorescence microscopy).**
White arrows indicate the direction of aerosol distribution.

Depth of tissue penetration measurements in the eIBUB are usually performed in triplicate (three measures (orange lines) in three tissue sections of three different biopsies at the exact location (top, middle, and bottom), totalizing nine biopsies, 27 tissue sections, and 81 measurements.

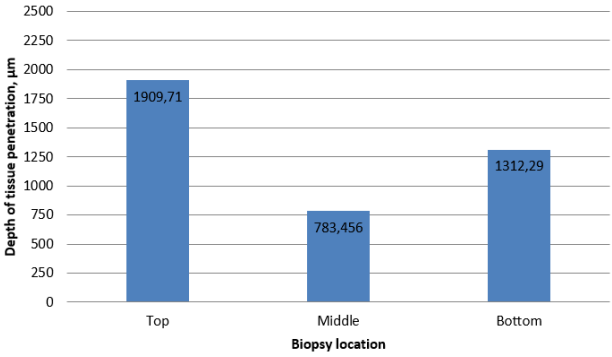

***Figure 15*: The mean depth of doxorubicin penetration.**

The mean depth of doxorubicin penetration after PIPAC in µm at the top, middle and bottom of the ex vivo eIBUB model.

Figure 15 depicts that the highest depth of doxorubicin penetration, 1909.71 µm, was at the top of eIBUB. In the middle, the penetration depth was 783.46 µm and at the bottom 1312.29 µm. The highest and lowest depth difference is 1126.25 µm or 60%. It demonstrates inhomogeneous spatial penetration of doxorubicin.

3.4.2 Measurement of liquid tissue uptake in real-time

Tissue uptake of the therapeutic solution was defined as the bladder weight gain over time, when the liquid falling was continuously removed. Two methods are available to calculate the liquid uptake into the peritoneal tissue:

- Indirectly, by calculating the difference between the aerosolized volume and the volume of the liquid falling:

  Volume of the liquid uptake (ml) = Volume of the sprayed liquid (ml) – Volume of the liquid collected in the communicating vessel (ml)

- Directly, by measuring the bladder weight gain according to the following equation [177]:

Volume of the liquid uptake (ml) = (Bladder weight at T1 (mg) – Bladder weight at T0 (mg))

Our experimental results showed the measurements to be the same for both methods (the data set saved on the university clinic hard drive). The second method was selected because of its user-friendliness.

For example, we examined liquid tissue uptake of a typical PIPAC solution with cisplatin and doxorubicin. Six IBUBs underwent aerosol exposure for 6 + 30 minutes (aerosolization and exposure time). The volume of aerosolized drug solution was 200 ml at a flow of 0.7 ml/sec. Figure 16 shows the eIBUB weight gain in real-time relative to the initial eIBUB weight.

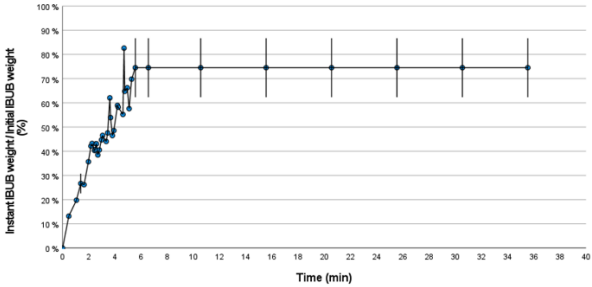

***Figure 16*: Tissue uptake of a cisplatin and doxorubicin solution as PIPAC in eIBUB model.**
The eIBUB weight increases by ¾ after aerosolization. Most liquid is taken up early, during the aerosolization phase (5 to 7 min).

The mean aerosolization time was 6.26 min. The bladder weight increased significantly by 74.5% ± 12.3% during aerosol application and then remained stable for the 30 minutes exposure.

3.4.2.1 Measurement of aerosol sedimentation in real-time

During PIPAC, a portion of the therapeutic solution falls to the bottom of the abdominal cavity. The causes are aerosol sedimenting (mainly by gravity and by impaction) and the

liquid solution dropping down the organ walls. In the eIBUB, the liquid is continuously collected and evacuated to a communicating vessel. The volume of fluid in this second vessel augments and can be determined in real-time. There are two ways of obtaining an objective measurement:

- By measuring its volume

The volume can be directly read from a scale printed on the plastic vessel. However, direct reading is not very precise. Digitalizing the volume data is possible but would be technically relatively challenging.

- By measuring its weight

The second vessel is placed on a scale with a digital output port [177]. After deduction of the tare, the weight can be measured easily with great precision.

For most aqueous solutions, the specific weight of the solution can be assumed to be equal to water (= 1).

In this study, aerosol sedimentation was measured with the weight method. Figure 17 depicts an example of a curve obtained with this method, showing the aerosol sedimenting over time in the eIBUB model, expressed in the percentage of the total drug volume aerosolized.

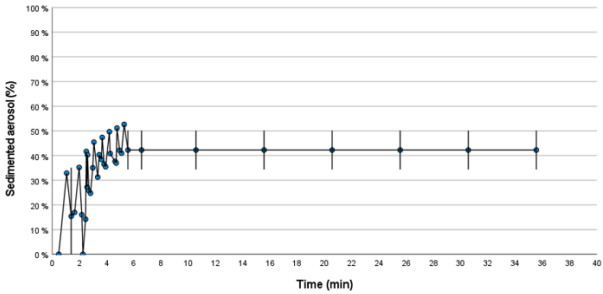

***Figure 17*: Aerosol sedimentation over time.**
Measurement of the aerosol sedimenting (or impacting) in the eIBUB model using the weight method. Error Bars: 95% CI.

The curve shows that the volume of the sedimented liquid increases rapidly during aerosolization (42.3 ± 8.0%) and then remains stable during the exposition phase (30 min) until the end of the procedure. Thus, aerosol uptake into the tissue during PIPAC occurs mainly during the phase of drug aerosolization. However, since 42% of the liquid precipitates at the bottom of the target organ, all the liquid aerosolized is not taken up into the tissue. Thus, there is an upper limit to the quantity of liquid from the aerosol that can be taken up by the tissue per time unit.

3.4.3 Financial requirements

The bovine urinary bladders were purchased from a registered slaughterhouse. The bladders were delivered to the lab by a taxi or a hospital transport vehicle. Costs are the following:

***Table 4*: Costs of the elBUB model.**

Position	Description	Time (min)	Costs (€)	Comments
1	Placing the order	5	3.75	Phone call by a technician
2	Transport costs		15	Lump-sum
3	Packaging including ice and reusable transport box		10	
4	Preparation time		21.6	Surgical resident
5	Trocar		20	Kii Applied Surgical
6	Silicone tubing section		0.5	20 cm
7	Connecting vessel		7	Can be reused
8	Use of laboratory equipment		50	Safety hood, balances, tripods, cleaning material, etc, lump-sum
	Total costs/elBUB		**97.85**	

3.4.4 Usability requirements

The working steps between reception of the organ from the slaughterhouse and the start of the experiment include:

Table 5: Usability requirements for the eIBUB model.

Step	Description	Time (min)	Comment
1	Inspecting the organ for lesions	1	Requires basic surgical competence
2	Dissecting fatty tissue and fascia	5	Needs basic surgical competence
3	Suturing the ureters	3	Requires basic surgical competence
3 4	Suturing a silicone tubing to the bladder base, connecting the communicating vessel	3	Requires basic surgical competence
5	Inverting the bladder through the bladder neck	2	

6	Inserting a trocar through the neck and placing a pursuing suture	5	Requires basic surgical competence
7	Suspending the bladder on a tripod	2	
8	Placing the communicating vessel in a scale	1	
9	Connecting the CO_2-insufflator	1	
	Total time	**24**	

Altogether, the time needed to verify the organ delivered and prepare the eIBUB model (until the effective start of the experiment) sums up to 24 minutes, which is 4 minutes over the specification.

3.4.5 Non-functional specifications

The pressure within the eIBUB is kept constant and monitored continuously via the CO_2-insufflator. In case of loss of pressure, the device insufflates immediately additional CO_2 to

maintain the desired pressure, In case of overpressure, the insufflator sound alarm and releases CO_2 into the environment. Then instant pressure is displayed on a screen, and are the instant insufflation flow and the total CO_2 volume insufflated since the beginning of the procedure.

The temperature within the eIBUB can be monitored continuously using, for example, a digital thermometer introduced into the trocar, or via a thermosensor introduced by punction through the eIBUB wall. The procedure can be video-monitored using an industry-standard, 5- or 10-mm laparoscopy camera.

We did not measure pH and humidity within the eIBUB. In theory, the intravesical pH can be easily monitored using a pH sensor placed within the eIBUB and connected to a recorder via a proper electronic interface. The sensor

can be placed through the trocar or via direct punction. Similarly, the intravesical relative humidity can be measured using a hygrometer. However, additional work is still needed to implement these additional measurement parameters, enabling multiparametric monitoring of the intravesical physico-chemical conditions over time.

To our knowledge, no powder formulation has been developed for intraperitoneal delivery. In contrast, intrapleural talcum delivery is an approved procedure for treating malignant pleural effusion. So far, we did no use the eIBUB model for optimizing delivery of undiluted powders.

Recent research has shown that the current Capnopen® technology does not allow aerosolization of thermolabile gels [181]. Thus,

we did not use the eIBUB model for evaluating the delivery of gels.

3.4.6 Verification of the specifications of the eIBUB model

Based on the results above, it is now possible to verify if the specifications defined ahead of time are met for the eIBUB model.

Table 6 summarizes the individual specifications and the corresponding verifications available to date.

***Table 6*: Verification of the specifications of the eIBUB model.**

Specifications		**Verification**	
Non-functional specifications	monitoring experimental parameters	pressure	Yes
		temperature	Yes
		humidity	Not verified
		pH	Not verified
		Video	Yes
Technical specifications	covered by peritoneum	Yes	
	creates a tight space	Yes	
	has a volume of 3-5 litres	Yes	
	can be expanded with a gas	CO_2	Yes
	tolerates an intraluminal pressure of up to 20 mmHg	Verified up to 15 mmHg	Yes
	collects the aerosol sedimenting / the liquid dripping down along the walls		Yes

	Video Graphics Array (VGA) offers a digital interface for real-time data collection		Yes
Environmental specifications	can be used within a safety laboratory hood		Yes
	has a closed aerosol waste system (CAWS)		Yes
Interaction specifications	application of liquids	Yes	
	application of gels	Not verified	
	application of powders	Not verified	
	various aerosolizing devices	Capnopen®	Yes
		Capnotip®	Yes
		Topol ®	Yes
		usPIPAC	Yes
	Various environments	PIPAC	Yes
		ePIPAC	Yes
		hPIPAC	No

3.5 Validation of the eIBUB model

As shown in Table 7, the requirements for the eIBUB model were largely validated, but only for a limited number of substances.

Table 7: Validation of the requirements for the eIBUB model.

Requirements		**Verification**	
Functional requirements	tissue drug concentration	Platin-based drugs	Yes
		Anthracyclins	Yes
		Taxanes	Yes
	depth of tissue drug penetration	Platin-based drugs	Not verified
		Anthracyclins	Yes
		Curcumin	Yes
	homogeneity of spatial drug distribution	Platin-based drugs	Yes
		Anthracyclins	Yes
	the homogeneity of spatial drug distribution	Platin-based drugs	Yes
		Anthracyclins	Yes

	tissue liquid uptake in real-time	Yes	
	aerosol sedimentation in real-time	Yes	
Financial requirements	material costs below 100 € / experiment	15 € / bladder	Yes
Usability requirements	can be easily setup	< 20 min	Yes
	can be used by a trained laboratory technician	Not verified	
Ethical / regulatory requirement	No use of living animals	Yes	

It has to be noted that the available IBUB model was already able to deliver most functionalities defined in the list of requirements for the eIBUB. However, when results of the eIBUB were compared with those obtained in the IBUB model, the experimental outcome was found to differ between the models.

- in the IBUB model, the aerosol falling remains at the base of the organ. The cumulated effects of the aerosol and the liquid are measured [177],
- in the eIBUB, the liquid collecting at the bottom of the organ is removed in real-time. Thus, only the effect of the aerosol is measured [177].

This difference is relevant since, over time, any aerosol is sedimenting due to gravitation forces. Thus, in the IBUB model, tissue drug concentration and depth or tissue penetration at the bottom of the organ are expected to increase over time, introducing a bias in the experiment results (overestimation). Moreover, the IBUB model underestimates the homogeneity of spatial distribution (as it is, also, in animal models). No such increase occurs in the eIBUB model.

The third and fourth functionalities are new: the eIBUB model was expected to provide researchers with additional knowledge on real-time tissue uptake of the therapeutic substance and the amount of therapeutic aerosol falling to the bottom of the target organ [177].

The methodology of the current study permits experiments to be conducted under safety conditions and the amount of organ material to be minimized. In addition, the discrepancy in statistics can be overcome in real-time experiments with one bladder per experiment. Moreover, the cost-effectiveness and applicability of the new model were demonstrated in practice.

For validation purposes, the accuracy and the precision of the data from experiments in the eIBUB model were compared with results

obtained in the animal model and in the human patient. Results are summarized in Table 8.

Table 8. Drug tissue concentration in the enhanced Inverted Bovine Urinary Bladder (eIBUB) model vs. gold standard (animal models and the human patient).

Author	Model	Drug	Tissue concentration (ng/mg)
Sautkin et al. [177]	eIBUB	DOX	18.5 ± 22.6
		CIS	10.6
Davigo et al. [125]	Swine	CIS	8.02 ± 9.1
Giger-Pabst et al. [158]	Swine	OX	37.16 ± 5.8
Solass et al. [124]	Human patient	DOX	1.7 ± 1.45
Tempfer et al. [182]	Human patient	DOX	19.2 ± 38.6
		CIS	131.5 ± 134.4

Only parietal biopsies were selected for this comparison. Since clinical biopsies are taken from the antero-lateral abdominal wall, we compared the human data with the data

obtained from the superior biopsies in the eIBUB. The concentration of doxorubicin in the eIBUB is comparable to peritoneal biopsies in the human patient. There is a large variability in the drug tissue concentration measured in animal models.

3.5.1 Measurement of the depth of drug tissue penetration

There is plenty of data on the depth of tissue penetration of doxorubicin ex-vivo, in the animal model and the human patient allowing to validate the eIBUB model (Table 9).

Table 9: Doxorubicin tissue penetration in the enhanced Inverted Bovine Urinary Bladder (eIBUB) model vs. gold standard (animal models and the human patient).

Author	Model	Location	Depth of tissue penetration (µm)
Sautkin et al. [177]	eIBUB	Parietal	433 (381-486)
Khosrawipour et al. [170]		Stomach	17 ± 17; 37 ± 28

	Swine post-mortem	Small intestine	311 ± 59; 349 ± 65
		Parietal	≤ 349 ± 65
Khosrawipour et al. [169]	Swine post-mortem	Small intestine	348; 312; 265
		Liver	64; 55; 40
Mimouni et al. [165]	Sheep post-mortem	Parietal/Visceral	> 100
Solass et al. [124]	Human patient	Parietal	~ 500

There is a good agreement between the depth of doxorubicin tissue penetration in the eIBUB vs. parietal peritoneum in the gold standard. However, in the animal model, the depth of drug tissue penetration has been found to differ widely between organs and localizations. For example, the depth of penetration of doxorubicin in the swine post-mortem was wide-ranging, between 17 µm on the surface of the stomach and 348 µm in the small intestine. Thus, results obtained in the eIBUB with biopsies of the parietal peritoneum might not be extrapolated to the visceral peritoneum.

Moreover, the variation in the measures appears to be smaller in the eIBUB than in the animal models. For example, the depth of doxorubicin varied by a factor two between individual animals in a post-mortem study in the pig [170].

3.5.2 Variability of measurements in the eIBUB model vs. available comparators

In the eIBUB model, the peritoneal samples are taken as punch biopsies and thus have a standardized diameter and a constant surface / depth ratio. To our knowledge, there is no study in the animal model where the sample geometry was standardized. The same observation applies to the human patient where biopsies are usually taken with endoscopic forceps, resulting in peritoneal lacerations with undetermined size and geometry. However, a recent study has shown the importance of

standardizing the sample geometry and the preanalytical sample preparation in peritoneal pharmacological studies [183].

We also compared the reproducibility of tissue drug concentration of cisplatin and doxorubicin between the eIBUB and the available IBUB model. As Table 10 is showing, differences in drug concentration were larger when multiple biopsies (n=12–42) from different bladders vs. biopsies from the same bladder (n=23) were compared [177].

***Table 10*: Variability of measured cisplatin and doxorubicin concentration in the eIBUB model vs. available comparator (IBUB model) [177].**

	Between urinary bladders				Same urinary bladder			
Position	Cisplatin	Sign.	Doxorubicin	Sign.	Cisplatin	Sign.	Doxorubicin	Sign.
Top	17.5 (13.6-21.4)	0.001*	0.7 (0.4-1.0)	0.10	15.0 (9.7-20.3)	0.77	0.8 (0.3-1.2)	0.25

Middle	7.3 (4.5-10.0)	0.002*	0.3 (0.0-0.6)	0.04*	12.8 (7.5-18.1)	0.94	0.4 (0.2-0.7)	0.93
Bottom	7.0 (3.5-10.6)	0.06	0.3 (0.1-0.4)	0.03*	12.8 (8.2-17.5)	0.87	0.4 (0.2-0.7)	0.63

Mean; CI 5–95%. ANOVA; *significant difference ($p<0.05$). Values (in ng/mg) are normalized to allow comparison.

Thus, the quality and reliability of the collection and analysis of tissue biopsies in the eIBUB model is at least equivalent to the available comparators, and probably superior to these comparators.

3.5.3 Outcome comparison between IBUB vs. eIBUB models

In the IBUB and the eIBUB model, biopsies are taken at the top, middle, and bottom of the organ. A comparison of tissue drug penetration and concentration is possible between different anatomical localizations. Thus, the IBUB and the eIBUB model enable the determination of

the homogeneity of spatial drug distribution [177].

For example, we measured the homogeneity of the spatial distribution of cisplatin after PIPAC (12 mmHg, 30 min, Capnopen® device) by measuring its tissue concentrations at different locations using the IBUB model.

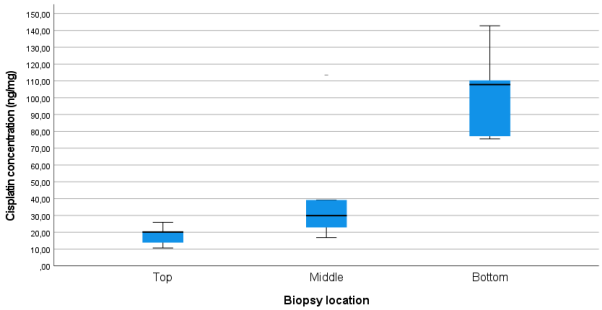

***Figure 18:* Homogeneity of cisplatin spatial distribution (as PIPAC) in the IBUB model.**
There is an increasing concentration gradient of cisplatin from the top to the bottom of the IBUB. The spatial distribution of cisplatin is not homogeneous. ANOVA, $p < 0.001$).

Cisplatin concentration was not homogeneous. The highest median cisplatin concentration was

at the bottom of the IBUBs (107.86 ng cisplatin/mg dry tissue), and the lowest at the top (20.14 ng/mg). The difference in concentration between the bottom and the top was 87.72 ng/mg ($p < 0.001$), between the bottom and the middle 77.92 ng/mg ($p = 0.008$) and between the middle and the top 9.8 ng/mg ($p = 0.045$).

In the IBUB model, these measures reflect the combined effect of the floating aerosol and the liquid collecting at the model's base. The same experiment was repeated in the eIBUB model, where solely the effect of the aerosol is measured (Figure 19).

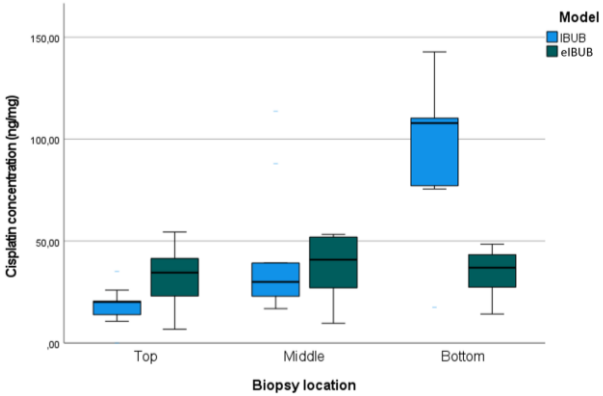

***Figure 19*: Homogeneity of cisplatin spatial distribution (as PIPAC) in the eIBUB model.**
In contrast to measurements in the IBUB model, no tissue drug concentration gradient is noted, and the spatial distribution of cisplatin within the organ walls is homogeneous.

Clearly, the results obtained differ between the IBUB and the eIBUB model, although the same experimental conditions were used. Thus, the choice of the model influences the quantitative measurements. Ideally, combining IBUB and eIBUB model measurements allows determining the relative effect of the aerosol vs. the liquid falling on drug tissue concentration. The combined results showed that, at the

model's base, the impact of the liquid falling on tissue drug uptake was superior to the effect of the aerosol, with a mean difference of 70.93 ng cisplatin / mg tissue (+ 65.8 %, $p < 0.001$). In contrast, the cisplatin tissue concentration at the top of the organ was significantly less in the IBUB than in the eIBUB model (- 41.7%, $p = 0.025$). There was no significant difference in the cisplation tissue concentration in the middle portion of the organ ($p = 0.63$).

4 Discussion

One particular avenue for developing more effective therapies for patients with peritoneal metastasis is to optimize intraperitoneal drug delivery. Intraperitoneal drug delivery as pressurized aerosols is a relatively new research field in contrast to pulmonary medicine. For example, impactors for examining nature and content of aerosol drugs in lung medicine have been developed as early as 1860 [177]. These impactors relied on a simple principle — a jet of particle-laden air impinging on a plate. The more sophisticated cascade impactor was discovered in the early 1950s and, along with extensive theoretical analysis of jet impaction, allowed significant progress in medical aerosols [184]. In pulmonary medicine, nebulizers used are submitted to a strict control and their performance has to be validated, in particular in

terms of drug mass delivered and the aerosol size distribution. The European standard EN 13544-1 specifies the requirements for nebulising systems which generate an aerosol for drug delivery to humans, through the respiratory organs [185].

In peritoneal medicine, the literature available on aerosolized drugs is scarce and most of it has been generated by our own research group. There is no standard or norm available for this application of nebulizing systems. This absence of references and guidelines is indeed a significant challenge for developing new drug delivery systems for treating patients with peritoneal diseases.

4.1 Current research landscape in intraperitoneal drug delivery

The current research landscape in intraperitoneal drug delivery can be classified into three main areas:

- Developing second-generation medical devices. For example, spatial homogeneity might be enhanced by using multi-head or rotating spraying devices [186].
- Optimizing drug formulations. For example, mucoadhesive polymers might improve the contact time between the aerosol and the peritoneum [181]; nanoparticles might prolong drug delivery [187, 188].
- Modifying the environment. Environmental control, e.g., electrostatic aerosol charging, might improve drug tissue uptake and homogeneity [161].

A combination of these approaches might create synergies. For example, the combination of the positive charge and electrostatic precipitation have significant potential to improve tissue uptake of nanoparticles during intraperitoneal chemotherapy [189].

As a consequence, research on intraperitoneal drug delivery has to consider several aspects to be successful:

- Device-related aspects, such as design, size, safety, material, compatibility with the formulation, and performance characteristics.
- Formulation variables, including active ingredients, excipients, compatibility with the device, flowability, uniformity, and stability
- Process parameters, such as micronization (droplet / particle size), droplet / particle morphology, moisture,

occupational health safety, in-process control, primary / protective packaging, control strategy, etc..

Thus, optimizing intraperitoneal drug delivery needs to consider several parameters at once and this R&D process occurs within a multidimensional research space with a higher level of complexity. The product and process development is guided by “Product Critical Quality Attributes” (CQA). CQAs are physical, chemical, biological, and microbiological properties or characteristics that have to be maintained within appropriate limits to ensure the desired product quality [190].

To obtain a first glimpse of the effect of a single variable within this research space, it is possible to perform simulations. For example, a computational fluid dynamic model was used to investigate whereas electrostatic precipitation

significantly improves spatial distribution during PIPAC [161].

4.2 Different functional peritoneal models for different research questions

As a complement to simulations in-silico, experiments are the most efficient tool to understand and quantitate the effects various parameters on the product's CQA. These experiments can be physical, chemical, pharmacological and biological, and are usually performed in functional models. In-vitro, ex-vivo, and in-vivo experimental models are available for optimizing intraperitoneal drug delivery.

In *vitro* cell culture models are often the first option for functional and pharmacological studies in peritoneal medicine. Cell culture

models allow toxicity, molecular and biological studies. These models are reproducible, cost-effective, and do not require animal sacrifice. However, two-dimensional cellular models do not reflect the complexity of the human peritoneal tissue. Hopefully, rapidly developing 3D cell culture [191] and cell printing technologies [192] will help create in-vitro models similar to the lining of the human abdominal cavity.

An *ex vivo* hermetic plastic box model [129], the first and simplest peritoneal model developed in peritoneal medicine, does not require animal sacrifices either, is cost-effective and highly reproducible. Experiments can be performed with normal or diseased human tissue samples. The plastic box model is easy to use, even in a laboratory with limited technical infrastructure and know-how. However, only a small fraction of the inner surface of the plastic box is lined

with mesothelium, which is a significant limiting feature for absorption studies.

Animal models in the mice, rat, rabbit and the swine offer an anatomy similar to the human abdominal cavity. They permit experiments both in healthy and diseased animals. Animal models are reproducible when they involve syngeneic animals. However, *in vivo* mice, rat, rabbit and swine models entail animal sacrificing for experiment purposes that ideally should be avoided [149]. Before beginning the experiment, regulatory approval must be obtained. Furthermore, experiments with animals call for trained staff, veterinarian support, special husbandry and care conditions [151, 155, 175]. The setup for *in vivo* swine, rat and rabbit models is complex and long-lasting as compared to other models. All these factors negatively affect the costs of the experiment. Moreover, the small size of rodents does not

allow easy used of standard PIPAC technology. Key CQA such as the intraperitoneal pressure and the volume of solution aerosolized have to be adapted, making extrapolation of the results to the human challenging. Nonetheless, *in vivo* swine, rat and rabbit models are still the best models for pharmacological studies for intraperitoneal drug delivery.

The (inverted) bovine urinary bladder (IBUB) model proposed by Schnelle et al. [149] was a significant advance for preclinical aerosol studies. The IBUB is an innovative and versatile ex vivo model for optimizing drug delivery with therapeutic aerosols both onto the mucosa or the serosa. This model can be used for pharmaceutical Quality-by-Design approaches and already replaced numerous animal studies. However, the IBUB model does not allow experiments in real-time or over time for the investigation of tissue aerosol absorption,

aerosol sedimentation, or free liquid formation. Thus, the IBUB model is not very helpful when the aim is to improve the formulation, for example prolonging the contact time with the tissue by using mucoadhesive polymers.

The following Table compares the features of the various peritoneal models available.

***Table 11*: Comparison of the peritoneal models available.**

Parameters	Cell culture	Plastic box	IBUB	eIBUB	Animal models
Model type	*in vitro*	*ex vivo*	*ex vivo*	*ex vivo*	*in vivo*
Degree of performance	-	-	-	++	-
Real-time aerosol sedimentation	-	-	-	++	-
Real-time tissue drug absorption	-	-	-	++	-
Similarity to human	-	-	+	+	++

abdominal cavity					
Tissue biopsies can be taken	+	++	+	++	++
Animal sacrifice necessary	-	-	-	-	++
Sophisticated model setup	+	+	+	+	++
Reproducibility	++	++	+	+	+
Cost-effectiveness	+	++	++	++	-

Legend: IBUB: inverted bovine urinary bladder; eIBUB: enhanced IBUB; - low performance; + moderate performance; ++ high performance.

The information above can be used to select a model particularly well suited for answering the research question.

4.3 The eIBUB model is a significant advance in peritoneal pharmacological research

The enhanced IBUB model (eIBUB) proposed in this thesis enables, for the first time in peritoneal medicine, the investigation of tissue drug saturation, aerosol sedimentation, and of tissue aerosol absorption in real-time. Such real-time measurement is, to our knowledge, not possible in animal models. Since the eIBUB now allows accurarte modelisation of the aerosol behavior and drug tissue uptake during PIPAC, it is a significant methodological advance in peritoneal medicine.

4.3.1 Real-time measurement of aerosol sedimentation

Real-time aerosol sedimentation reflects how much of the aerosol is sedimenting as a free liquid. In other words, real-time measurement of

aerosol sedimentation shows how much aerosol does not reach the target tissue. Since this aerosol fraction is not absorbed by the target tissue, it should, in principle, not contribute to the therapeutic effect.

However, the aerosol sedimenting collects a liquid at the bottom of the target cavity and this liquid collecting is in contact with the peritoneum. Some tissue absorption of this liquid is expected, which might be significant or even superior to the effect of the aerosol elsewhere. In fact, the therapeutic solution collecting at the bottom is in contact with the target organ during the whole exposure time and even after the procedure, since no liquid is removed at the end of PIPAC. A longer exposure time increases indeed the probability that more therapeutic solution will penetrate the tissue. Thus, during and after PIPAC, the therapeutic solution penetrates the tissue in the

most decline part of the abdomen, and creates a vertical concentration gradient.

In the eIBUB model, collection of free liquid in the communicating vessel can be measured in real-time by monitoring its weight [177] or its volume. Once aerosol spraying is completed, the difference between the volume of the solution aerosolized and the volume of liquid collected in the second vessel reflects the volume of solution absorbed by the target tissue. This study shows that, during PIPAC, aerosol sedimentation and free liquid formation occur mostly during aerosol application and then the system remains stable until the end of the exposure time.

The peritoneal tissue has limited ability to take up fluids. Intuitively, the situation can be compared to a heavy rainfall and the risk of flooding when the soil cannot absorb all the

water within a short period of time. In analogy, when the flow aerosolized is higher than the tissue liquid uptake capacity, no further absorption is possible and the aerosol droplets drip down along the peritoneal lining, In the eIBUB model, the maximal tissue saturation can be observed when the first droplets of the sedimented aerosol start to collect in the communicating vessel. The volume / weight increase in the communicating vessel reflects the volume aerosolized beyond the maximal tissue absorption threshold.

In contrast to the eIBUB, other models such as the *in-vitro* cell culture model, the ex-vivo hermetic plastic box and IBUB model, and the *in vivo* mice, rat, rabbit and swine models permit aerosol sedimentation to be measured only at the end of the experiment. These models cannot demonstrate the exact volume of the sedimented aerosol and cannot distinguish

between the target effect of the aerosol vs. liquid.

Lack of knowledge of the above features can lead to a false interpretation of experimental results, For example, in an animal study with Tc99 in four swines, planar scintigraphy showed inhomogeneous nuclide distribution post-mortem [167]. After PIPAC, only 8–10% of the delivered nuclide was detected in one region of interest with a considerable deviation from a uniform nuclide distribution pattern. SPECT/CT revealed ‘‘hot spots’’ in the cul-de-sac region (the lowest part of the abdomen in the supine position). The authors concluded that “intra-abdominal aerosol distribution pattern of PIPAC therapy is non-homogeneous and that the currently applied technology has still not overcome the problem of inhomogeneous drug distribution of intraperitoneal chemotherapy”. In fact, they

obviously did not measure aerosol distribution but the volume of liquid sedimenting.

The eIBUB model has highlighted that the target effect of the therapeutic solution during PIPAC depends on two components: the aerosol and a liquid fraction. However, the respective therapeutic effect of the aerosol (during PIPAC) vs. the collected liquid (during and after PIPAC) remains unclear at this stage. This is in contrast to HIPEC, where no postoperative effect is expected since the abdomen is washed out with physiological solution at the end of the procedure [193].

4.3.2 Tissue aerosol absorption

Real-time tissue aerosol absorption measurement demonstrates how much aerosol penetrates the target tissue during an experiment and can be observed in the eIBUB model [177]. A correlation can be established

between the organ (in our study: the urinary bladder) volume and weight, on the one hand, and the amount of aerosol absorbed by organ, on the other hand. Moreover, data concerning organ volume and weight make it possible to calculate the tissue density using the formula:

$$\rho = \frac{\mathrm{m}}{\mathrm{V}},$$

where “m” is IBUB weight before experiment and “V” is IBUB volume.

Secondly, in the eIBUB model, a correlation can be defined between tissue density and the amount of aerosol absorbed. In clinical practice, tissue density can be measured by elastometry, which is a well known non-invasive ultrasound-based method for measurement of the stiffness of organs such as liver, breast, prostate, lymph nodes etc. [194]. In this study, the bladder

weight was measured before the experiment and its volume with a graduated cylinder filled with water. The difference in the water volume before and after placing the bladder into the cylinder shows the volume of the bladder. Thus, the bladder weight and volume permit tissue density to be calculated with the aforementioned formula. Data regarding the aerosol uptake into the bladder can be compared with its calculated tissue density to further establish a correlation between these parameters. Knowing the correlation between bladder tissue density and aerosol absorption, the optimal volume, respectively the maximal flow of the spray solution can be calculated in advance for each bladder and each specific substance to be aerosolized.

In the eIBUB model, during aerosol application, the sedimented liquid is drawn off countinuously into a second vessel, preventing

liquid collection at the bottom of the bladder [177]. If the sedimented liquid is not removed from the target organ, it will overlay the target tissue and exert a therapeutic effect in addition to the aerosol. By calculating the ideal volume, respectively the maximal flow of the spray solution for each bladder, the volume of sedimented liquid can be reduced or aerosol sedimentation might even be completely avoided. In analogy, this principle might be applied to human abdomens of different sizes and peritoneal absorption surfaces.

Thus, in contrast to other available models, the eIBUB model allows a precise calculation aerosolization parameters (volume and flow) and thus can prevent aerosol sedimentation and sedimented liquid collection in the target cavity. Thus, the eIBUB is the only model permitting the aerosol effects on the target

tissue to be investigated since the target tissue is exposed only to the aerosol.

However, precise calculation of the spray solution volume and flow does not guarantee that the whole therapeutic solution will be absorbed by the target tissue, because other factors influence tissue drug absorption such as, for instance, freshness of the biological material or the age of the animal from which the target tissue was obtained. These additional factors are not completely clear and demand more attention. Nonetheless, even if aerosol sedimentation occurs after precisely calculating the solution volume, the amount of liquid collecting at the bottom of the target organ is expected to be smaller than in experiments where the volume of the spray solution is not calculated. Consequently, the eIBUB is the only model that permits the collection of sedimented liquid to be completely avoided during

therapeutic aerosol application, while at the same time it is irrelevant whether the volume of the spray solution was specifically calculated for the target organ or not.

The accumulation of the sedimented liquid in the communicating vessel can be used for further correction of the spray volume, flow, technology optimization, and the development of advanced formulations enhancing the contract time between the aerosol and the peritoneum.

By defining the correlation between target tissue density and aerosol absorption, the eIBUB model can help to reduce the amount of sedimented liquid in the human abdominal cavity following PIPAC. Consequently, exposure of the target tissue to the aerosol might be optimized. Thus, the eIBUB model opens new research avenues for optimizing

intraperitoneal drug delivery as pressurized aerosols.

4.4 Pharmacological outcomes differ between IBUB and eIBUB models

We have observed that, under the same experimental conditions, the measured pharmacological outcome in the eIBUB model differs from the IBUB model. Differences were found for tissue drug concentration and for depth of drug tissue penetration.

4.4.1 Tissue drug concentration

Quantitative analyses of tissue drug concentration in the eIBUB model showed a relatively homogeneous distribution of doxorubicin and cisplatin throughout the target tissue. Only minor, non-significant differences were measured: the highest tissue drug concentration was achieved in the middle, the

lowest at the top of the bladders. At the bottom of the bladders, the drug concentration was somewhat higher than at the top.

In the IBUB model proposed by Schnelle et al. the cisplatin tissue concentration at the bottom of IBUBs was the highest and was approximately three times higher than the concentration measured at the top, middle, and bottom of the eIBUB model. This difference can be explained by the collection of sedimented liquid at the bottom of IBUB during aerosol application and, later on, during the exposure time. The presence of free liquid can lead to drug uptake into the tissue. This is probably the reason for significantly higher cisplatin concentration at the bottom of IBUB model than in the eIBUB model.

4.4.2 Depth of drug tissue penetration

The eIBUB model demonstrated the highest depth of drug penetration at the top of the bladder, where tissue exposure to aerosol is maximal. Conversely, the middle part of the bladder, with the highest exposure to sedimented liquid, showed the lowest drug penetration, proving superior aerosol penetration to fluid.

The differences in measurement of tissue drug concentration and depth of drug tissue penetration are all but a surprise since the eIBUB model is designed to measure the target effect of the therapeutic aerosol alone, whereas, in the IBUB model, the aerosol and the liquid's combined effects are evaluated. The aerosol falling to the bottom of the target organ has, by definition, no or little effect on the remaining peritoneal tissue. This liquid accumulating at the bottom might increase drug

concentration and drug tissue penetration, exerting there an effect independent of the aerosol.

Against this background, it is essential to recognize that the choice of the model (eIBUB vs. IBUB) will influence the results obtained in the target tissue. This fact needs to be considered in the interpretation of data.

4.5 The eIBUB model fulfills most requirements and specifications

The large majority of the non-functional, technical and environmental specifications of the eIBUB model have been verified successfully in appropriate experiments. Exceptions are the ability to monitor the relative humidity and pH within the eIBUB during the experiments. Such monitoring should be easily

possible with industry-standard hygrometers and pH meters.

The application of gels and powders has not yet been tested in the eIBUB, and challenges can be expected:

- in the interaction of gels with the device,
- possible clotting of the aerosol powder in an environment highly saturated with humidity.

However, in the absence of experimental proof, it is not possible at this stage to conclude on the suitability of eIBUB for optimizing intraperitoneal drug delivery with gels or dry powder formulations.

4.6 Validation of the eIBUB model: can the results be extrapolated to the clinical situation?

The experimental data comprise the standard against which the eIBUB outputs are compared.

In the case of intraperitoneal drug delivery, the gold standard is the human patent or, in the case such data is not available, data obtained in a living, large animal model.

Using precisely the same key quality attributes (device, drug concentration, volume of solution, pressure, exposition time), cisplatin tissue concentration after PIPAC was rather heterogeneous in the IBUB model and rather homogeneous in the eIBUB model. The clinical significance of the concentration gradient between the top and the bottom of the IBUB, respectively the anterior wall of the abdomen and the visceral organs in the patient's supine position, remains undetermined. On the one hand, it is logical to seek a homogeneous distribution of the therapeutic aerosol in the peritoneal cavity. On the other hand, most organs are located on the bottom of the abdomen when the patient lies in

the supine position. A maximal impregnation of these organs, in particular of the small bowel, with the therapeutic solution, might be a worthwhile goal.

In any case, our compared results in the IBUB and eIBUB models underline the causal role of the liquid collecting at the lowest location of the target organ in augmenting local tissue drug concentration, a phenomenon probably occurring in the clinical situation. The respective therapeutic effect of the aerosol during PIPAC vs. the collected liquid after PIPAC remains unclear at this stage. This is in contrast to HIPEC, where the abdomen is usually washed out with physiological solution at the end of the procedure [193].

During the validation process, not only the absolute value but also the uncertainty in the measured quantities should be estimated. In

this study, we showed that the variability of biological results is significantly lower within a single bladder (using the eIBUB as a model) than between different bladders (using the IBUB as a model) [177]. The variability of pharmacological measurements in the target tissue appears lower than reported in animal models [125, 158, 170].

The results of this study highlight that the model choice is crucial for optimizing intraperitoneal drug delivery since results can differ depending on the model. Taken together, the extrapolation of findings from the eIBUB model to the human patient is credible.

4.7 Limitations of the eIBUB model

Beside all its advantages, the IBUB model has also several limtations.

- The eIBUB only permits the study of normal peritoneal tissue, as opposed to diseased, e.g. tumoral tissue [177].
- The eIBUB model is not vascularized and does not allow pharmacokinetics and pharmacodynamics studies [177].
- *In-vivo* results obtained in the swine model, and, to a lesser degree, in the rat and rabbit, are better transferable to the human organism because of anatomical and physiological similarities.
- The tissue might be autolytic. Fresh bladders should be obtained from the slaughterhouse and immediately transported on ice to the laboratory to prevent autolysis and tissue degradation.
- Assessment of the biological effect of a given drug on the target tissue is barely possible with the eIBUB [177], the

observation window being limited to a few hours.

- The eIBUB setup is more complicated than for the plastic box model. The tubing inserted at the bottom of the IBUB is associated with a higher risk for CO_2 leakage. Thus, experiments using the eIBUB require technical expertise and there is a learning curve.

To reduce the variability in the results, bladders selected for the experiment should have nearly the same weight, length, volume, and wall thickness.

4.8 Future research directions

We expect the eIBUB model to be increasingly adopted by the academic research community. However, before results obtained in the eIBUB model are accepted by certifying bodies (for medical delices) and regulatory authorities (for

drugs and formulations), further validation work might be needed. A certification if the model and related procedures (e.g. according to ISO-DIN) will probably be required by the industry. The amount of work and the precise content will then be determined in an adequate project plan.

As explained above, the respective therapeutic effect of the aerosol during PIPAC vs. the collected liquid after PIPAC remains unclear at this stage. Research comparing results in the IBUB and eIBUB will be crucial for elucidating this effect, and this research will be needed for each drug-device combination in order to determine the optimal CQA. These CQA will need to consider not only the device and the formulation, but also the volume aerosolized. Obviously, there is an upper limit to the quantity of liquid from the aerosol that can be taken up by the tissue per time unit. Consequence for

devices development, increasing aerosolization flow might have negative effects.

Against this framework, the clinical significance of the drug concentration gradient between the top and the bottom of the IBUB, respectively the anterior wall of the abdomen and the visceral organs in the patient's supine position, remains also undetermined. Since the abdominal organs, in particular the small bowel, are located in the decline part of the abdomen when the patient lies in supine position, and since the surface of the visceral peritoneum exceeds the surface of the parietal peritoneum, some distribution gradient might have positive effect.

We expect the eIBUB model to be crucial in the optimization process of electrostatic precipitation PIPAC (ePIPAC), in particular for determining the time point of activation of the device and the minimal application time to

reach a drug tissue concentration at least equivalent to PIPAC after 30 min.

During the implementation and validation phases, the eIBUB has already allowed unexpected observations and insights on the target effect of drugs aerosolized into the abdomen. With increasing use of the eiBUB in the research community, we expect this model to enable significant observations in the understanding of intraperitoneal drug delivery and thus to facilitate the development of effective therapies for patients with peritoneal metastasis.

5 Summary (EN)

Pressurized IntraPeritoneal Aerosol Chemotherapy (PIPAC) is a minimally invasive treatment mode for local chemotherapy of Peritoneal Metastasis (PM). PIPAC has demonstrated promising results in the first clinical studies. Optimization of the current drug-devices combinations requires functional models. The currently used *in vivo, in vitro* and *ex vivo* models cannot deliver real-time information on tissue drug uptake. Moreover, alternatives should be developed to limit research on living animals.

This study focuses on the development and validation of an ex vivo model for optimizing intraperitoneal drug delivery, the enhanced Inverted Bovine Urinary Bladder Model (eIBUB). The research builds up on the IBUB model proposed by Schnelle et al in 2017, by

connecting a second vessel to the bladder. A list of specifications and requirements for an ex-vivo model was created.

The eIBUB model takes advantage of the principle of communicating vessels by connecting the base of the bladder to a second, hermetic container kept under an identical pressure. This design allows continuous collection of the aerosol falling down, and real-time assessment of the tissue liquid uptake (i.e., the portion of the therapeutic aerosol effectively taken up by the tissue) vs. the liquid falling down (which, by definition, can only have a limited therapeutic effect). This study details the technical setup of the eIBUB model and its feasibility, in particular concerning real-time measurements. The verification process showed that the eIBUB model meets the majority of the specifications. The usability and safety of the eIBUB model was confirmed under

real laboratory conditions using toxic drugs. The validation process, involving two drugs commonly used during PIPAC (doxorubicin and cisplatin), showed that the depth of tissue penetration and the tissue drug concentration are in line with the gold standard (measurements in the human patient) and available comparators (ex-vivo and animal models). The variability of the results was at least comparable to the comparators. The eIBUB model meets the ARRIVE criteria (replacement, reduction, refinement) in animal research. Thus, the eIBUB model is a significant advance in peritoneal pharmacological research.

6 Summary (DE)

Pressurized IntraPeritoneal Aerosol Chemotherapy (PIPAC) ist ein minimalinvasives Behandlungsverfahren zur lokalen Chemotherapie und kommt bei peritonealen Metastasen (PM) zur Anwendung. In den ersten klinischen Studien hat die PIPAC vielversprechende Ergebnisse gezeigt. Die Optimierung der Kombination von Medikament-Gerät erfordert ein funktionelles Model. Die heutzutage verwendeten in vivo, in vitro und ex vivo Modelle liefern keine Informationen über die Absorption von Aerosolen im Gewebe in Echtzeit. Darüber hinaus sollen alternative Modelle entwickelt werden, um die Forschung am lebenden Tiermodell zu minimieren.

Diese Studie fokussiert sich auf die Entwicklung und Validierung eines ex vivo Modells, das die intraperitoneale Verabreichung von

Medikamenten optimiert und wird „Verbessertes invertiertes Rinderharnblasen Modell (eIBUB)“ genannt. Die Studie basiert auf dem Model, das von Schnelle et al. im Jahr 2017 vorgeschlagen wurde, indem ein zusätzliches Gefäß mit der Rinderharnblase verbunden wurde. Es wurde eine Liste mit Spezifikationen und Anforderungen für ein ex vivo Modell erstellt.

Das eIBUB Modell nützt die Vorteile des Prinzips der kommunizierenden Röhren, indem der Boden der, wobei Rinderharnblase mit einem zweiten dicht verschlossenen Gefäß unter dem gleichen Druck verbunden wird. Dieses Design ermöglicht die kontinuierliche Sammlung von herunterfallendem Aerosol und die Echtzeit Evaluierung der Absorption von Flüssigkeiten im Gewebe (d.h., die Menge von therapeutischem Aerosol, das vom Gewebe effizient absorbiert wurde) vs. herunterfallender

Flüssigkeit (die per Definition nur eingeschränkte therapeutische Wirkungen haben kann). Diese Studie zeigt im Detail das technische Setup sowie die Durchführbarkeit des eIBUB Modells, insbesondere die Messungen in Echtzeit betreffend. Der Verifizierungsprozess hat gezeigt, dass das eIBUB Modell die Mehrheit von Spezifikationen erfüllt hat. Die Anwendbarkeit und Sicherheit des eIBUB Models wurden unter echten Laborbedingungen unter Verwendung von toxischen Medikamenten bestätigt. Der Validierungprozess hat mit der Applikation von zwei der am häufigsten verwendeten Medikamente für die PIPAC (Doxorubicin and Cisplatin) gezeigt, dass die Eindringtiefe im Gewebe und die Konzentration im Gewebe auf einer Linie mit dem Gold Standard (Messungen an Patienten) und mit den verfügbaren Komparatoren (ex vivo und Tiermodelle)

stehen. Die Vielschichtigkeit der Ergebnisse war mindestens vergleichbar mit den Komparatoren. Das eIBUB Model entspricht den ARRIVE Kriterien (Vermeiden, Verringern, Verbessern) hinsichtlich Tierversuchen.

Daher leistet das eIBUB Modell einen signifikanten Beitrag in der peritonealen pharmakologischen Forschung.

7 Bibliography

1. His W, *Die Häute und Höhlen des Körpers*. 1865, Schweighauserische Universitäts-Buchdruckerei: Basel. p. 1-34.
2. Bichat X, *A treatise on the membranes in general, and of different membranes in particular*. 1813, Cummings and Hilliard: Boston. p. 73-105.
3. Minot C, *The mesoderm and the coelom of vertebrates.* 1890. **24**(286): p. 877-898.
4. Maksimenkov A, *Surgical Anatomy of the Abdomen*. 1972: Leningrad. p. 85.
5. Albanese AM, Albanese EF, Miño JH, Gómez E, Gómez M, Zandomeni M, and Merlo AB, *Peritoneal surface area: measurements of 40 structures covered by peritoneum: correlation between total peritoneal surface area and the surface calculated by formulas.* Surgical and Radiologic Anatomy, 2009. **31**(5): p. 369-377.
6. Philipp S, Jan Philipp R, Daniel N, Klaus E, and Tarkan J, *The PEritoneal SUrface CAlculator (PESUCA): A new tool to quantify the resected peritoneal surface area after cytoreductive surgery.* Pleura and Peritoneum, 2020. **5**(1): p. 20190031.
7. Standring S, *Gray's anatomy : the anatomical basis of clinical practice*. 2016.
8. Hanbidge AE, Lynch D, and Wilson SR, *US of the peritoneum.* Radiographics, 2003. **23**(3): p. 663-84; discussion 684-5.

9. Wilkosz S, Ireland G, Khwaja N, Walker M, Butt R, de Giorgio-Miller A, and Herrick SE, *A comparative study of the structure of human and murine greater omentum.* Anat Embryol (Berl), 2005. **209**(3): p. 251-61.
10. Blackburn SC and Stanton MP, *Anatomy and physiology of the peritoneum.* Semin Pediatr Surg, 2014. **23**(6): p. 326-30.
11. Platell C, Cooper D, Papadimitriou JM, and Hall JC, *The omentum.* World J Gastroenterol, 2000. **6**(2): p. 169-176.
12. Bloom W and Maximow A, *A Textbook of Histology*. 1952: Philadelphia. p. 34.
13. Michailova K, Wassilev W, and Wedel T, *Scanning and transmission electron microscopic study of visceral and parietal peritoneal regions in the rat.* Annals of Anatomy - Anatomischer Anzeiger, 1999. **181**(3): p. 253-260.
14. Ackermann PC, De Wet PD, and Loots GP, *Microcirculation of the rat omentum studied by means of corrosion casts.* Acta Anat (Basel), 1991. **140**(2): p. 146-9.
15. Shimotsuma M, Kawata M, Hagiwara A, and Takahashi T, *Milky spots in the human greater omentum. Macroscopic and histological identification.* Acta Anat (Basel), 1989. **136**(3): p. 211-6.
16. Zhu H, Naito M, Umezu H, Moriyama H, Takatsuka H, Takahashi K, and Shultz LD, *Macrophage differentiation and expression of macrophage colony-stimulating factor in*

murine milky spots and omentum after macrophage elimination. J Leukoc Biol, 1997. **61**(4): p. 436-44.
17. Solass W, Horvath P, Struller F, Konigsrainer I, Beckert S, Konigsrainer A, Weinreich FJ, and Schenk M, *Functional vascular anatomy of the peritoneum in health and disease.* Pleura Peritoneum, 2016. **1**(3): p. 145-158.
18. Aune S, *Transperitoneal exchange. II. Peritoneal blood flow estimated by hydrogen gas clearance.* Scandinavian journal of gastroenterology, 1970. **5**(2): p. 99-104.
19. Granger DN, Ulrich M, Perry MA, and Kvietys PR, *Peritoneal dialysis solutions and feline splanchnic blood flow.* Clin Exp Pharmacol Physiol, 1984. **11**(5): p. 473-81.
20. Guyton A and Hall J, *Local and humoral control of blood flow by the tissues.*, in *Textbook of medical physiology*. 2006, Elsevier Saunders: Philadephia. p. 195–203.
21. Bock R. *Virtuelle Mikroskopie. Anat. Inst. Luebeck.* 28.04.2007 [cited 21.02.2021]; Appendix (Mensch). Faerbung Masson-Goldner]. Available from: https://mikroskopie-uds.de/.
22. Wang NS, *The regional difference of pleural mesothelial cells in rabbits.* Am Rev Respir Dis, 1974. **110**(5): p. 623-33.
23. Mironov VA, Gusev SA, and Baradi AF, *Mesothelial stomata overlying omental milky*

spots: Scanning electron microscopic study. Cell and Tissue Research, 1979. **201**(2): p. 327-330.

24. Leak LV and Rahil K, *Permeability of the diaphragmatic mesothelium: the ultrastructural basis for "stomata".* Am J Anat, 1978. **151**(4): p. 557-93.
25. Gotloib L, Shostack A, and Jaichenko J, *Ruthenium-red-stained anionic charges of rat and mice mesothelial cells and basal lamina: the peritoneum is a negatively charged dialyzing membrane.* Nephron, 1988. **48**(1): p. 65-70.
26. O'Rahilly R and Müller F. *Abdominal Viscera*. Basic human anatomy : a regional study of human structure 1983 [cited 13.08.2020]; Available from: https://www.dartmouth.edu/~humananatomy/part_5/chapter_26.html.
27. Kenny HA, Krausz T, Yamada SD, and Lengyel E, *Use of a novel 3D culture model to elucidate the role of mesothelial cells, fibroblasts and extra-cellular matrices on adhesion and invasion of ovarian cancer cells to the omentum.* Int J Cancer, 2007. **121**(7): p. 1463-72.
28. Topley N, Petersen MM, Mackenzie R, Neubauer A, Stylianou E, Kaever V, Davies M, Coles GA, Jörres A, and Williams JD, *Human peritoneal mesothelial cell prostaglandin synthesis: induction of cyclooxygenase mRNA*

by peritoneal macrophage-derived cytokines. Kidney Int, 1994. **46**(3): p. 900-9.
29. Ha H, Cha MK, Choi HN, and Lee HB, *Effects of peritoneal dialysis solutions on the secretion of growth factors and extracellular matrix proteins by human peritoneal mesothelial cells.* Perit Dial Int, 2002. **22**(2): p. 171-7.
30. Yung S, Thomas GJ, Stylianou E, Williams JD, Coles GA, and Davies M, *Source of peritoneal proteoglycans. Human peritoneal mesothelial cells synthesize and secrete mainly small dermatan sulfate proteoglycans.* Am J Pathol, 1995. **146**(2): p. 520-9.
31. van der Wal BC, Hofland LJ, Marquet RL, van Koetsveld PM, van Rossen ME, and van Eijck CH, *Paracrine interactions between mesothelial and colon-carcinoma cells in a rat model.* Int J Cancer, 1997. **73**(6): p. 885-90.
32. Tavianatou AG, Caon I, Franchi M, Piperigkou Z, Galesso D, and Karamanos NK, *Hyaluronan: molecular size-dependent signaling and biological functions in inflammation and cancer.* Febs j, 2019. **286**(15): p. 2883-2908.
33. Casey RC and Skubitz AP, *CD44 and beta1 integrins mediate ovarian carcinoma cell migration toward extracellular matrix proteins.* Clin Exp Metastasis, 2000. **18**(1): p. 67-75.
34. Hausmann MJ, Rogachev B, Weiler M, Chaimovitz C, and Douvdevani A, *Accessory role of human peritoneal mesothelial cells in*

antigen presentation and T-cell growth. Kidney Int, 2000. **57**(2): p. 476-86.
35. Zegera Gd, *Fibrinolysis*, in *The Peritoneum*. 1992, Springer-Verlag: New York. p. 209-210.
36. Whitaker D and Papadimitriou J, *Mesothelial healing: morphological and kinetic investigations.* J Pathol, 1985. **145**(2): p. 159-75.
37. Raftery AT, *Regeneration of parietal and visceral peritoneum in the immature animal: a light and electron microscopical study.* Br J Surg, 1973. **60**(12): p. 969-75.
38. Jacquet P, Vidal-Jove J, Zhu B, and Sugarbaker P, *Peritoneal carcinomatosis from gastrointestinal malignancy: natural history and new prospects for management.* Acta chirurgica Belgica, 1994. **94**(4): p. 191-197.
39. Flanagan M, Solon J, Chang KH, Deady S, Moran B, Cahill R, Shields C, and Mulsow J, *Peritoneal metastases from extra-abdominal cancer - A population-based study.* Eur J Surg Oncol, 2018. **44**(11): p. 1811-1817.
40. Tsai JH and Yang J, *Epithelial-mesenchymal plasticity in carcinoma metastasis.* Genes Dev, 2013. **27**(20): p. 2192-206.
41. Yin M, Li X, Tan S, Zhou HJ, Ji W, Bellone S, Xu X, Zhang H, Santin AD, Lou G, and Min W, *Tumor-associated macrophages drive spheroid formation during early transcoelomic metastasis of ovarian cancer.* The Journal of

clinical investigation, 2016. **126**(11): p. 4157-4173.
42. Cunliffe WJ and Sugarbaker PH, *Gastrointestinal malignancy: rationale for adjuvant therapy using early postoperative intraperitoneal chemotherapy.* Br J Surg, 1989. **76**(10): p. 1082-90.
43. Sugarbaker PH, *A perspective on clinical research strategies in carcinoma of the large bowel.* World J Surg, 1991. **15**(5): p. 609-16.
44. Terzi C, Arslan NC, and Canda AE, *Peritoneal carcinomatosis of gastrointestinal tumors: where are we now?* World journal of gastroenterology, 2014. **20**(39): p. 14371-14380.
45. Levy AD, Shaw JC, and Sobin LH, *Secondary tumors and tumorlike lesions of the peritoneal cavity: imaging features with pathologic correlation.* Radiographics, 2009. **29**(2): p. 347-73.
46. Odendahl K, Solass W, Demtröder C, Giger-Pabst U, Zieren J, Tempfer C, and Reymond MA, *Quality of life of patients with end-stage peritoneal metastasis treated with Pressurized IntraPeritoneal Aerosol Chemotherapy (PIPAC).* Eur J Surg Oncol, 2015. **41**(10): p. 1379-85.
47. Sadeghi B, Arvieux C, Glehen O, Beaujard AC, Rivoire M, Baulieux J, Fontaumard E, Brachet A, Caillot JL, Faure JL, Porcheron J, Peix JL, François Y, Vignal J, and Gilly FN, *Peritoneal carcinomatosis from non-gynecologic*

malignancies: results of the EVOCAPE 1 multicentric prospective study. Cancer, 2000. **88**(2): p. 358-63.

48. Montori G, Coccolini F, Ceresoli M, Catena F, Colaianni N, Poletti E, and Ansaloni L, *The Treatment of Peritoneal Carcinomatosis in Advanced Gastric Cancer: State of the Art.* International Journal of Surgical Oncology, 2014. **2014**: p. 912418.
49. Dromain C, Leboulleux S, Auperin A, Goere D, Malka D, Lumbroso J, Schumberger M, Sigal R, and Elias D, *Staging of peritoneal carcinomatosis: enhanced CT vs. PET/CT.* Abdom Imaging, 2008. **33**(1): p. 87-93.
50. Low RN, Barone RM, and Lucero J, *Comparison of MRI and CT for predicting the Peritoneal Cancer Index (PCI) preoperatively in patients being considered for cytoreductive surgical procedures.* Ann Surg Oncol, 2015. **22**(5): p. 1708-15.
51. Graniel-Palafox LE and Guerrero-Avendaño G, *Vías de diseminación y sitios frecuentes de implantación metastásica en carcinomatosis peritoneal; hallazgos por tomografía.* Anales de Radiologia, Mexico, 2013. **12**(1): p. 29-35.
52. Koh JL, Yan TD, Glenn D, and Morris DL, *Evaluation of preoperative computed tomography in estimating peritoneal cancer index in colorectal peritoneal carcinomatosis.* Ann Surg Oncol, 2009. **16**(2): p. 327-33.

53. Fehniger J, Thomas S, Lengyel E, Liao C, Tenney M, Oto A, and Yamada SD, *A prospective study evaluating diffusion weighted magnetic resonance imaging (DW-MRI) in the detection of peritoneal carcinomatosis in suspected gynecologic malignancies.* Gynecol Oncol, 2016. **142**(1): p. 169-175.
54. Klumpp BD, Schwenzer N, Aschoff P, Miller S, Kramer U, Claussen CD, Bruecher B, Koenigsrainer A, and Pfannenberg C, *Preoperative assessment of peritoneal carcinomatosis: intraindividual comparison of 18F-FDG PET/CT and MRI.* Abdom Imaging, 2013. **38**(1): p. 64-71.
55. De Blasis I, Moruzzi MC, Moro F, Mascilini F, Cianci S, Gueli Alletti S, Turco LC, Garganese G, Scambia G, and Testa AC, *Role of ultrasound in advanced peritoneal malignancies.* Minerva Med, 2019. **110**(4): p. 292-300.
56. Duffy MJ, van Dalen A, Haglund C, Hansson L, Holinski-Feder E, Klapdor R, Lamerz R, Peltomaki P, Sturgeon C, and Topolcan O, *Tumour markers in colorectal cancer: European Group on Tumour Markers (EGTM) guidelines for clinical use.* Eur J Cancer, 2007. **43**(9): p. 1348-60.
57. Goonetilleke KS and Siriwardena AK, *Systematic review of carbohydrate antigen (CA 19-9) as a biochemical marker in the diagnosis of pancreatic cancer.* Eur J Surg Oncol, 2007. **33**(3): p. 266-70.

58. Medeiros LR, Rosa DD, da Rosa MI, and Bozzetti MC, *Accuracy of CA 125 in the diagnosis of ovarian tumors: a quantitative systematic review.* Eur J Obstet Gynecol Reprod Biol, 2009. **142**(2): p. 99-105.
59. Garofalo A and Valle M, *Laparoscopy in the management of peritoneal carcinomatosis.* Cancer J, 2009. **15**(3): p. 190-5.
60. Laterza B, Kusamura S, Baratti D, Oliva GD, and Deraco M, *Role of explorative laparoscopy to evaluate optimal candidates for cytoreductive surgery and hyperthermic intraperitoneal chemotherapy (HIPEC) in patients with peritoneal mesothelioma.* In Vivo, 2009. **23**(1): p. 187-90.
61. Iversen LH, Rasmussen PC, and Laurberg S, *Value of laparoscopy before cytoreductive surgery and hyperthermic intraperitoneal chemotherapy for peritoneal carcinomatosis.* Br J Surg, 2013. **100**(2): p. 285-92.
62. Pomel C, Appleyard TL, Gouy S, Rouzier R, and Elias D, *The role of laparoscopy to evaluate candidates for complete cytoreduction of peritoneal carcinomatosis and hyperthermic intraperitoneal chemotherapy.* Eur J Surg Oncol, 2005. **31**(5): p. 540-3.
63. Hentzen J, van der Plas WY, Constansia RDN, Been LB, Hoogwater FJH, van Ginkel RJ, van Dam GM, Hemmer PHJ, and Kruijff S, *Role of diagnostic laparoscopy in patients with suspicion of colorectal peritoneal metastases to*

evaluate suitability for cytoreductive surgery with hyperthermic intraperitoneal chemotherapy. BJS Open, 2019. **3**(6): p. 812-821.

64. Valle M and Garofalo A, *Laparoscopic staging of peritoneal surface malignancies.* Eur J Surg Oncol, 2006. **32**(6): p. 625-7.
65. Jacquet P and Sugarbaker PH, *Clinical research methodologies in diagnosis and staging of patients with peritoneal carcinomatosis.* Cancer Treat Res, 1996. **82**: p. 359-74.
66. Tentes AA, Tripsiannis G, Markakidis SK, Karanikiotis CN, Tzegas G, Georgiadis G, and Avgidou K, *Peritoneal cancer index: a prognostic indicator of survival in advanced ovarian cancer.* Eur J Surg Oncol, 2003. **29**(1): p. 69-73.
67. Jayakrishnan TT, Zacharias AJ, Sharma A, Pappas SG, Gamblin TC, and Turaga KK, *Role of laparoscopy in patients with peritoneal metastases considered for cytoreductive surgery and hyperthermic intraperitoneal chemotherapy (HIPEC).* World journal of surgical oncology, 2014. **12**: p. 270-270.
68. Harmon RL and Sugarbaker PH, *Prognostic indicators in peritoneal carcinomatosis from gastrointestinal cancer.* Int Semin Surg Oncol, 2005. **2**(1): p. 3.
69. Solass W, Sempoux C, Detlefsen S, Carr NJ, and Bibeau F, *Peritoneal sampling and histological assessment of therapeutic response in*

peritoneal metastasis: proposal of the Peritoneal Regression Grading Score (PRGS). Pleura Peritoneum, 2016. **1**(2): p. 99-107.

70. Demtröder C, Giger-Past U, Solass W, and Reymond M, *Therapy of Peritoneal Carcinomatosis*, in *PIPAC Pressurized Intraperitoneal Aerosol Chemotherapy - Cancer under Pressure*, M. Reymond and W. Solass, Editors. 2014, De Gruyter: Germany. p. 35.
71. Demtröder C, Giger-Pabst U, Solass W, and Reymond M, *Systemic Palliative Chemotherapy*, in *PIPAC Pressurized Intraperitoneal Aerosol Chemotherapy - Cancer under Pressure*, M. Reymond and W. Solass, Editors. 2014, De Gruyter: Germany. p. 35-36.
72. Verwaal VJ, Ruth Sv, Bree Ed, Slooten GWv, Tinteren Hv, Boot H, and Zoetmulder FAN, *Randomized Trial of Cytoreduction and Hyperthermic Intraperitoneal Chemotherapy Versus Systemic Chemotherapy and Palliative Surgery in Patients With Peritoneal Carcinomatosis of Colorectal Cancer.* Journal of Clinical Oncology, 2003. **21**(20): p. 3737-3743.
73. Khomiakov V, Meisner C, Ryabov A, Bolotina L, Utkina A, Kolobaev I, Sobolev D, and Chayka A, *Palliative systemic chemotherapy with or without pressurized intraperitoneal aerosol chemotherapy with cisplatin and doxorubicin (PIPAC C/D) for gastric cancer with peritoneal metastasis: A propensity score analysis.* Journal

of Clinical Oncology, 2020. **38**(4_suppl): p. 380-380.

74. Somashekhar SP, Ashwin KR, Rauthan A, and Rohit C, *Pressurized IntraPeritoneal Aerosol Chemotherapy vs. intravenous chemotherapy for unresectable peritoneal metastases secondary to platinum resistant ovarian cancer – study protocol for a randomized control trial.* Pleura and Peritoneum, 2019. **4**(1).

75. Lavoue V, Huchon C, Akladios C, Alfonsi P, Bakrin N, Ballester M, Bendifallah S, Bolze PA, Bonnet F, Bourgin C, Chabbert-Buffet N, Collinet P, Courbiere B, De la Motte Rouge T, Devouassoux-Shisheboran M, Falandry C, Ferron G, Fournier L, Gladieff L, Golfier F, Gouy S, Guyon F, Lambaudie E, Leary A, Lecuru F, Lefrere-Belda MA, Leblanc E, Lemoine A, Narducci F, Ouldamer L, Pautier P, Planchamp F, Pouget N, Ray-Coquard I, Rousset-Jablonski C, Senechal-Davin C, Touboul C, Thomassin-Naggara I, Uzan C, You B, and Daraï E, *Management of epithelial cancer of the ovary, fallopian tube, and primary peritoneum. Short text of the French Clinical Practice Guidelines issued by FRANCOGYN, CNGOF, SFOG, and GINECO-ARCAGY, and endorsed by INCa.* Eur J Obstet Gynecol Reprod Biol, 2019. **236**: p. 214-223.

76. Bazarbashi S, Hakoun AM, Gad AM, Elshenawy MA, Aljubran A, Alzahrani AM, and Eldali A, *Efficacy of second-line chemotherapy after a*

first-line triplet in patients with metastatic colorectal cancer. Curr Oncol, 2019. **26**(1): p. e24-e29.

77. Good DJ, Polverini PJ, Rastinejad F, Le Beau MM, Lemons RS, Frazier WA, and Bouck NP, *A tumor suppressor-dependent inhibitor of angiogenesis is immunologically and functionally indistinguishable from a fragment of thrombospondin.* Proc Natl Acad Sci U S A, 1990. **87**(17): p. 6624-8.
78. Maione TE, Gray GS, Petro J, Hunt AJ, Donner AL, Bauer SI, Carson HF, and Sharpe RJ, *Inhibition of angiogenesis by recombinant human platelet factor-4 and related peptides.* Science, 1990. **247**(4938): p. 77.
79. Liu X, Nie W, Xie Q, Chen G, Li X, Jia Y, Yin B, Qu X, Li Y, and Liang J, *Endostatin reverses immunosuppression of the tumor microenvironment in lung carcinoma.* Oncology letters, 2018. **15**(2): p. 1874-1880.
80. O'Reilly MS, Holmgren L, Shing Y, Chen C, Rosenthal RA, Moses M, Lane WS, Cao Y, Sage EH, and Folkman J, *Angiostatin: A novel angiogenesis inhibitor that mediates the suppression of metastases by a lewis lung carcinoma.* Cell, 1994. **79**(2): p. 315-328.
81. O'Reilly MS, Boehm T, Shing Y, Fukai N, Vasios G, Lane WS, Flynn E, Birkhead JR, Olsen BR, and Folkman J, *Endostatin: An Endogenous Inhibitor of Angiogenesis and Tumor Growth.* Cell, 1997. **88**(2): p. 277-285.

82. Selbonne S, Azibani F, Iatmanen S, Boulaftali Y, Richard B, Jandrot-Perrus M, Bouton M-C, and Arocas V, *In vitro and in vivo antiangiogenic properties of the serpin protease nexin-1.* Molecular and cellular biology, 2012. **32**(8): p. 1496-1505.
83. Franko J, Shi Q, Meyers JP, Maughan TS, Adams RA, Seymour MT, Saltz L, Punt CJA, Koopman M, Tournigand C, Tebbutt NC, Diaz-Rubio E, Souglakos J, Falcone A, Chibaudel B, Heinemann V, Moen J, De Gramont A, Sargent DJ, and Grothey A, *Prognosis of patients with peritoneal metastatic colorectal cancer given systemic therapy: an analysis of individual patient data from prospective randomised trials from the Analysis and Research in Cancers of the Digestive System (ARCAD) database.* Lancet Oncol, 2016. **17**(12): p. 1709-1719.
84. Gremonprez F, Descamps B, Izmer A, Vanhove C, Vanhaecke F, De Wever O, and Ceelen W, *Pretreatment with VEGF(R)-inhibitors reduces interstitial fluid pressure, increases intraperitoneal chemotherapy drug penetration, and impedes tumor growth in a mouse colorectal carcinomatosis model.* Oncotarget, 2015. **6**(30): p. 29889-900.
85. Zhao ZX, Li X, Liu WD, Liu XZ, Wu SJ, and Hu XH, *Inhibition of Growth and Metastasis of Tumor in Nude Mice after Intraperitoneal Injection of Bevacizumab.* Orthop Surg, 2016. **8**(2): p. 234-40.

86. Jordan K, Luetkens T, Gog C, Killing B, Arnold D, Hinke A, Stahl M, Freier W, Rüssel J, Atanackovic D, and Hegewisch-Becker S, *Intraperitoneal bevacizumab for control of malignant ascites due to advanced-stage gastrointestinal cancers: A multicentre double-blind, placebo-controlled phase II study - AIO SUP-0108.* Eur J Cancer, 2016. **63**: p. 127-34.
87. Bell RB, Fernandes RP, and Andersen PE, *Surgery and Immunotherapy*, in *Oral, Head and Neck Oncology and Reconstructive Surgery*, R.B. Bell, R.P. Fernandes, and P.E. Andersen, Editors. 2018, Elsevier. p. 919-943.
88. Mizumoto A, Canbay E, Hirano M, Takao N, Matsuda T, Ichinose M, and Yonemura Y, *Morbidity and Mortality Outcomes of Cytoreductive Surgery and Hyperthermic Intraperitoneal Chemotherapy at a Single Institution in Japan.* Gastroenterology Research and Practice, 2012. **2012**: p. 836425.
89. Kapoor S, Bassily-Marcus A, Alba Yunen R, Tabrizian P, Semoin S, Blankush J, Labow D, Oropello J, Manasia A, and Kohli-Seth R, *Critical care management and intensive care unit outcomes following cytoreductive surgery with hyperthermic intraperitoneal chemotherapy.* World J Crit Care Med, 2017. **6**(2): p. 116-123.
90. Passot G, Bakrin N, Roux AS, Vaudoyer D, Gilly FN, Glehen O, and Cotte E, *Quality of life after cytoreductive surgery plus hyperthermic intraperitoneal chemotherapy: a prospective*

study of 216 patients. Eur J Surg Oncol, 2014. **40**(5): p. 529-535.

91. Rovers KP, Bakkers C, Simkens GAAM, Burger JWA, Nienhuijs SW, Creemers G-JM, Thijs AMJ, Brandt-Kerkhof ARM, Madsen EVE, Ayez N, de Boer NL, van Meerten E, Tuynman JB, Kusters M, Sluiter NR, Verheul HMW, van der Vliet HJ, Wiezer MJ, Boerma D, Wassenaar ECE, Los M, Hunting CB, Aalbers AGJ, Kok NFM, Kuhlmann KFD, Boot H, Chalabi M, Kruijff S, Been LB, van Ginkel RJ, de Groot DJA, Fehrmann RSN, de Wilt JHW, Bremers AJA, de Reuver PR, Radema SA, Herbschleb KH, van Grevenstein WMU, Witkamp AJ, Koopman M, Haj Mohammad N, van Duyn EB, Mastboom WJB, Mekenkamp LJM, Nederend J, Lahaye MJ, Snaebjornsson P, Verhoef C, van Laarhoven HWM, Zwinderman AH, Bouma JM, Kranenburg O, van 't Erve I, Fijneman RJA, Dijkgraaf MGW, Hemmer PHJ, Punt CJA, Tanis PJ, de Hingh IHJT, Dutch Peritoneal Oncology G, and Dutch Colorectal Cancer G, *Perioperative systemic therapy and cytoreductive surgery with HIPEC versus upfront cytoreductive surgery with HIPEC alone for isolated resectable colorectal peritoneal metastases: protocol of a multicentre, open-label, parallel-group, phase II-III, randomised, superiority study (CAIRO6).* BMC cancer, 2019. **19**(1): p. 390-390.

92. van Driel WJ, Koole SN, Sikorska K, Schagen van Leeuwen JH, Schreuder HWR, Hermans RHM,

de Hingh I, van der Velden J, Arts HJ, Massuger L, Aalbers AGJ, Verwaal VJ, Kieffer JM, Van de Vijver KK, van Tinteren H, Aaronson NK, and Sonke GS, *Hyperthermic Intraperitoneal Chemotherapy in Ovarian Cancer.* N Engl J Med, 2018. **378**(3): p. 230-240.

93. Virzì S, Iusco D, Bonomi S, and Grassi A, *Hyperthermic Intraperitoneal Chemotherapy (HIPEC) Techniques*, in *Treatment of Peritoneal Surface Malignancies. Updates in Surgery*, G. A. and P. E., Editors. 2015, Springer: Milan, Italy. p. 155-168.
94. Burnett A, Lecompte M-EA, Trabulsi N, Dubé P, Gervais M-K, Trilling B, Cloutier A-S, and Sideris L, *Peritoneal carcinomatosis index predicts survival in colorectal patients undergoing HIPEC using oxaliplatin: a retrospective single-arm cohort study.* World journal of surgical oncology, 2019. **17**(1): p. 83-83.
95. Ceelen W, *HIPEC with oxaliplatin for colorectal peritoneal metastasis: The end of the road?* Eur J Surg Oncol, 2019. **45**(3): p. 400-402.
96. Sugarbaker P, *Early Postoperative Intraperitoneal Chemotherapy*, in *Treatment of Peritoneal Surface Malignancies. State of the Art and Perspectives*, A. Giorgio and E. Pinto, Editors. 2015, Springer-Verlag: Italy, Milan. p. 97.
97. Feuer DDJ and Broadley KE. *Surgery for the resolution of symptoms in malignant bowel obstruction in advanced gynaecological and*

gastrointestinal cancer. Cochrane Database of Systematic Reviews 2000 [cited 15.08.2020]; Available from: https://doi.org//10.1002/14651858.CD002764.

98. Dunn D, Ganapathy S, and Chan V, *Surgical Palliation*, in *Surgical Palliative Care and Pain Management, An Issue of Anesthesiology Clinics*. 2012, Elsevier Health Science. p. 48-51.
99. Gwilliam B and Bailey C, *The nature of terminal malignant bowel obstruction and its impact on patients with advanced cancer.* Int J Palliat Nurs, 2001. **7**(10): p. 474-81.
100. Soriano A and Davis MP, *Malignant bowel obstruction: individualized treatment near the end of life.* Cleve Clin J Med, 2011. **78**(3): p. 197-206.
101. Ripamonti CI, Easson AM, and Gerdes H, *Management of malignant bowel obstruction.* Eur J Cancer, 2008. **44**(8): p. 1105-15.
102. Demtröder C, Giger-Pabst U, Solass W, and Reymond M, *Intraperitoneal Immunotherapy*, in *PIPAC Pressurized Intraperitoneal Aerosol Chemotherapy - Cancer under Pressure*, M. Reymond and W. Solass, Editors. 2014, De Gruyter. p. 50-52.
103. Dubovsky JA, Beckwith KA, Natarajan G, Woyach JA, Jaglowski S, Zhong Y, Hessler JD, Liu TM, Chang BY, Larkin KM, Stefanovski MR, Chappell DL, Frissora FW, Smith LL, Smucker KA, Flynn JM, Jones JA, Andritsos LA, Maddocks K, Lehman AM, Furman R, Sharman J, Mishra A,

Caligiuri MA, Satoskar AR, Buggy JJ, Muthusamy N, Johnson AJ, and Byrd JC, *Ibrutinib is an irreversible molecular inhibitor of ITK driving a Th1-selective pressure in T lymphocytes.* Blood, 2013. **122**(15): p. 2539-49.

104. Freedman RS, *Immunobiology and Intraperitoneal Immunobiologics in Ovarian Cancer*, in *Intraperitoneal Cancer Therapy*, C. Helm and R. Edwards, Editors. 2007, Humana Press: Totowa, New Jersey. p. 45-52.
105. Guo B, Fu S, Zhang J, Liu B, and Li Z, *Targeting inflammasome/IL-1 pathways for cancer immunotherapy.* Scientific reports, 2016. **6**: p. 36107-36107.
106. Hodi FS, O'Day SJ, McDermott DF, Weber RW, Sosman JA, Haanen JB, Gonzalez R, Robert C, Schadendorf D, Hassel JC, Akerley W, van den Eertwegh AJ, Lutzky J, Lorigan P, Vaubel JM, Linette GP, Hogg D, Ottensmeier CH, Lebbé C, Peschel C, Quirt I, Clark JI, Wolchok JD, Weber JS, Tian J, Yellin MJ, Nichol GM, Hoos A, and Urba WJ, *Improved survival with ipilimumab in patients with metastatic melanoma.* N Engl J Med, 2010. **363**(8): p. 711-23.
107. Oudard S, Rixe O, Beuselinck B, Linassier C, Banu E, Machiels JP, Baudard M, Ringeisen F, Velu T, Lefrere-Belda MA, Limacher JM, Fridman WH, Azizi M, Acres B, and Tartour E, *A phase II study of the cancer vaccine TG4010 alone and in combination with cytokines in patients with metastatic renal clear-cell*

carcinoma: clinical and immunological findings. Cancer Immunol Immunother, 2011. **60**(2): p. 261-71.

108. Liu L, Zhang W, Qi X, Li H, Yu J, Wei S, Hao X, and Ren X, *Randomized study of autologous cytokine-induced killer cell immunotherapy in metastatic renal carcinoma.* Clin Cancer Res, 2012. **18**(6): p. 1751-9.
109. Fry TJ, Shah NN, Orentas RJ, Stetler-Stevenson M, Yuan CM, Ramakrishna S, Wolters P, Martin S, Delbrook C, Yates B, Shalabi H, Fountaine TJ, Shern JF, Majzner RG, Stroncek DF, Sabatino M, Feng Y, Dimitrov DS, Zhang L, Nguyen S, Qin H, Dropulic B, Lee DW, and Mackall CL, *CD22-targeted CAR T cells induce remission in B-ALL that is naive or resistant to CD19-targeted CAR immunotherapy.* Nat Med, 2018. **24**(1): p. 20-28.
110. Zhou X, Mo X, Qiu J, Zhao J, Wang S, Zhou C, Su Y, Lin Z, and Ma H, *Chemotherapy combined with dendritic cell vaccine and cytokine-induced killer cells in the treatment of colorectal carcinoma: a meta-analysis.* Cancer management and research, 2018. **10**: p. 5363-5372.
111. Nowrousian MR, Waschke S, Bojko P, Welt A, Schuett P, Ebeling P, Flasshove M, Moritz T, Schuette J, and Seeber S, *Impact of chemotherapy regimen and hematopoietic growth factor on mobilization and collection of*

peripheral blood stem cells in cancer patients. Ann Oncol, 2003. **14 Suppl 1**: p. i29-36.

112. Tong Y, Song W, and Crystal RG, *Combined intratumoral injection of bone marrow-derived dendritic cells and systemic chemotherapy to treat pre-existing murine tumors.* Cancer Res, 2001. **61**(20): p. 7530-5.
113. Martuza RL, Malick A, Markert JM, Ruffner KL, and Coen DM, *Experimental therapy of human glioma by means of a genetically engineered virus mutant.* Science, 1991. **252**(5007): p. 854-6.
114. Field HJ and Wildy P, *The pathogenicity of thymidine kinase-deficient mutants of herpes simplex virus in mice.* J Hyg (Lond), 1978. **81**(2): p. 267-77.
115. Toda M, Martuza RL, and Rabkin SD, *Tumor Growth Inhibition by Intratumoral Inoculation of Defective Herpes Simplex Virus Vectors Expressing Granulocyte–Macrophage Colony-Stimulating Factor.* Molecular Therapy, 2000. **2**(4): p. 324-329.
116. Fawaz LM, Sharif-Askari E, and Menezes J, *Up-regulation of NK cytotoxic activity via IL-15 induction by different viruses: a comparative study.* J Immunol, 1999. **163**(8): p. 4473-80.
117. Nakao A, Kasuya H, Sahin TT, Nomura N, Kanzaki A, Misawa M, Shirota T, Yamada S, Fujii T, Sugimoto H, Shikano T, Nomoto S, Takeda S, Kodera Y, and Nishiyama Y, *A phase I dose-escalation clinical trial of intraoperative direct*

intratumoral injection of HF10 oncolytic virus in non-resectable patients with advanced pancreatic cancer. Cancer Gene Ther, 2011. **18**(3): p. 167-75.

118. Hu JC, Coffin RS, Davis CJ, Graham NJ, Groves N, Guest PJ, Harrington KJ, James ND, Love CA, McNeish I, Medley LC, Michael A, Nutting CM, Pandha HS, Shorrock CA, Simpson J, Steiner J, Steven NM, Wright D, and Coombes RC, *A phase I study of OncoVEXGM-CSF, a second-generation oncolytic herpes simplex virus expressing granulocyte macrophage colony-stimulating factor.* Clin Cancer Res, 2006. **12**(22): p. 6737-47.
119. Lauer UM, Schell M, Beil J, Berchtold S, Koppenhofer U, Glatzle J, Konigsrainer A, Mohle R, Nann D, Fend F, Pfannenberg C, Bitzer M, and Malek NP, *Phase I Study of Oncolytic Vaccinia Virus GL-ONC1 in Patients with Peritoneal Carcinomatosis.* Clin Cancer Res, 2018. **24**(18): p. 4388-4398.
120. Moehler M, Sieben M, Roth S, Springsguth F, Leuchs B, Zeidler M, Dinsart C, Rommelaere J, and Galle PR, *Activation of the human immune system by chemotherapeutic or targeted agents combined with the oncolytic parvovirus H-1.* BMC Cancer, 2011. **11**: p. 464.
121. Zou P, Tang R, and Luo M, *Oncolytic virotherapy, alone or in combination with immune checkpoint inhibitors, for advanced melanoma: A systematic review and meta-*

analysis. International Immunopharmacology, 2020. **78**: p. 106050.

122. Nadiradze G, Horvath P, Sautkin Y, Archid R, Weinreich F-J, Königsrainer A, and Reymond MA, *Overcoming Drug Resistance by Taking Advantage of Physical Principles: Pressurized Intraperitoneal Aerosol Chemotherapy (PIPAC).* Cancers, 2019. **12**(1): p. 34.
123. Solaß W, Hetzel A, Nadiradze G, Sagynaliev E, and Reymond MA, *Description of a novel approach for intraperitoneal drug delivery and the related device.* Surg Endosc, 2012. **26**(7): p. 1849-55.
124. Solass W, Kerb R, Mürdter T, Giger-Pabst U, Strumberg D, Tempfer C, Zieren J, Schwab M, and Reymond MA, *Intraperitoneal chemotherapy of peritoneal carcinomatosis using pressurized aerosol as an alternative to liquid solution: first evidence for efficacy.* Ann Surg Oncol, 2014. **21**(2): p. 553-9.
125. Davigo A, Passot G, Vassal O, Bost M, Tavernier C, Decullier E, Bakrin N, Alyami M, Bonnet J-M, Louzier V, Paquet C, Allaouchiche B, Glehen O, and Kepenekian V, *PIPAC versus HIPEC: cisplatin spatial distribution and diffusion in a swine model.* International Journal of Hyperthermia, 2020. **37**(1): p. 144-150.
126. Khomyakov V, Ryabov A, Ivanov A, Bolotina L, Utkina A, Volchenko N, and Kaprin A, *Bidirectional chemotherapy in gastric cancer with peritoneal metastasis combining*

intravenous XELOX with intraperitoneal chemotherapy with low-dose cisplatin and Doxorubicin administered as a pressurized aerosol: an open-label, Phase-2 study (PIPAC-GA2). Pleura Peritoneum, 2016. **1**(3): p. 159-166.

127. Hinds W, *Introduction*, in *Aerosol Technology: Properties, Behavior, and Measurement of Airborne Particles*. 1999, John Wiley and Sons: Canada. p. 22.
128. Reymond MA, Hu B, Garcia A, Reck T, Köckerling F, Hess J, and Morel P, *Feasibility of therapeutic pneumoperitoneum in a large animal model using a microvaporisator.* Surg Endosc, 2000. **14**(1): p. 51-5.
129. Solass W, Herbette A, Schwarz T, Hetzel A, Sun JS, Dutreix M, and Reymond MA, *Therapeutic approach of human peritoneal carcinomatosis with Dbait in combination with capnoperitoneum: proof of concept.* Surg Endosc, 2012. **26**(3): p. 847-52.
130. Kurtz F, Struller F, Horvath P, Solass W, #x00F6, sm, #x00FC, ller H, #x00F6, nigsrainer A, and Reymond MA, *Feasibility, Safety, and Efficacy of Pressurized Intraperitoneal Aerosol Chemotherapy (PIPAC) for Peritoneal Metastasis: A Registry Study %J Gastroenterology Research and Practice.* 2018. **2018**: p. 8.
131. Eveno C, Jouvin I, and Pocard M, *PIPAC EstoK 01: Pressurized IntraPeritoneal Aerosol*

Chemotherapy with cisplatin and doxorubicin (PIPAC C/D) in gastric peritoneal metastasis: a randomized and multicenter phase II study. Pleura Peritoneum, 2018. **3**(2): p. 20180116.

132. Solass W, Kerb R, Mürdter T, Giger-Pabst U, Strumberg D, Tempfer C, Zieren J, Schwab M, and Reymond MA, *Intraperitoneal chemotherapy of peritoneal carcinomatosis using pressurized aerosol as an alternative to liquid solution: first evidence for efficacy.* Annals of surgical oncology, 2014. **21**(2): p. 553-559.
133. Boltromejuck V, *Aerosol*, in *General Chemestry*. 2012, Vyschaia Shcola Minsk, Belarussia. p. 274.
134. *Gas pressure and molecule speed*. [cited 08.05.2019]; Available from: https://chem21.info/info/385405/.
135. Jacquet P, Stuart OA, Chang D, and Sugarbaker PH, *Effects of intra-abdominal pressure on pharmacokinetics and tissue distribution of doxorubicin after intraperitoneal administration.* Anticancer Drugs, 1996. **7**(5): p. 596-603.
136. Esquis P, Consolo D, Magnin G, Pointaire P, Moretto P, Ynsa MD, Beltramo JL, Drogoul C, Simonet M, Benoit L, Rat P, and Chauffert B, *High intra-abdominal pressure enhances the penetration and antitumor effect of intraperitoneal cisplatin on experimental*

peritoneal carcinomatosis. Ann Surg, 2006. **244**(1): p. 106-12.
137. Facy O, Al Samman S, Magnin G, Ghiringhelli F, Ladoire S, Chauffert B, Rat P, and Ortega-Deballon P, *High pressure enhances the effect of hyperthermia in intraperitoneal chemotherapy with oxaliplatin: an experimental study.* Ann Surg, 2012. **256**(6): p. 1084-8.
138. Heldin CH, Rubin K, Pietras K, and Ostman A, *High interstitial fluid pressure - an obstacle in cancer therapy.* Nat Rev Cancer, 2004. **4**(10): p. 806-13.
139. Nadiradze G, Horvath P, Sautkin Y, Archid R, Weinreich FJ, Königsrainer A, and Reymond MA, *Overcoming Drug Resistance by Taking Advantage of Physical Principles: Pressurized Intraperitoneal Aerosol Chemotherapy (PIPAC).* Cancers (Basel), 2019. **12**(1).
140. Schilling MK, Redaelli C, Krähenbühl L, Signer C, and Büchler MW, *Splanchnic microcirculatory changes during CO2 laparoscopy.* J Am Coll Surg, 1997. **184**(4): p. 378-82.
141. Solass W, Giger-Pabst U, Zieren J, and Reymond MA, *Pressurized intraperitoneal aerosol chemotherapy (PIPAC): occupational health and safety aspects.* Annals of surgical oncology, 2013. **20**(11): p. 3504-3511.
142. Alyami M, Hübner M, Grass F, Bakrin N, Villeneuve L, Laplace N, Passot G, Glehen O, and Kepenekian V, *Pressurised intraperitoneal*

aerosol chemotherapy: rationale, evidence, and potential indications. The Lancet Oncology, 2019. **20**(7): p. e368-e377.

143. Solass W, Giger-Pabst U, Zieren J, and Reymond MA, *Pressurized intraperitoneal aerosol chemotherapy (PIPAC): occupational health and safety aspects.* Ann Surg Oncol, 2013. **20**(11): p. 3504-11.
144. Grangeia HB, Silva C, Simões SP, and Reis MS, *Quality by design in pharmaceutical manufacturing: A systematic review of current status, challenges and future perspectives.* Eur J Pharm Biopharm, 2020. **147**: p. 19-37.
145. Steuperaert M, Falvo D'Urso Labate G, Debbaut C, De Wever O, Vanhove C, Ceelen W, and Segers P, *Mathematical modeling of intraperitoneal drug delivery: simulation of drug distribution in a single tumor nodule.* Drug Deliv, 2017. **24**(1): p. 491-501.
146. Weinreich J, Struller F, Sautkin I, Giuashvili S, Reymond M, Königsrainer A, and Schott TC, *Chemosensitivity of various peritoneal cancer cell lines to HIPEC and PIPAC: comparison of an experimental duplex drug to standard drug regimens in vitro.* Invest New Drugs, 2019. **37**(3): p. 415-423.
147. Khosrawipour V, Khosrawipour T, Diaz-Carballo D, Förster E, Zieren J, and Giger-Pabst U, *Exploring the Spatial Drug Distribution Pattern of Pressurized Intraperitoneal Aerosol*

Chemotherapy (PIPAC). Ann Surg Oncol, 2016. **23**(4): p. 1220-4.

148. Khosrawipour V, Khosrawipour T, Falkenstein TA, Diaz-Carballo D, Forster E, Osma A, Adamietz IA, Zieren J, and Fakhrian K, *Evaluating the Effect of Micropump(c) Position, Internal Pressure and Doxorubicin Dosage on Efficacy of Pressurized Intra-peritoneal Aerosol Chemotherapy (PIPAC) in an Ex Vivo Model.* Anticancer Res, 2016. **36**(9): p. 4595-600.
149. Schnelle D, Weinreich FJ, Kibat J, and Reymond MA, *A new ex vivo model for optimizing distribution of therapeutic aerosols: the (inverted) bovine urinary bladder.* Pleura Peritoneum, 2017. **2**(1): p. 37-41.
150. Eveno C, Haidara A, Ali I, Pimpie C, Mirshahi M, and Pocard M, *Experimental pharmacokinetics evaluation of chemotherapy delivery by PIPAC for colon cancer: first evidence for efficacy.* Pleura Peritoneum, 2017. **2**(2): p. 103-109.
151. Van de Sande L, Willaert W, Cosyns S, De Clercq K, Shariati M, Remaut K, and Ceelen W, *Establishment of a rat ovarian peritoneal metastasis model to study pressurized intraperitoneal aerosol chemotherapy (PIPAC).* BMC Cancer, 2019. **19**(1): p. 424.
152. *PubMed Research with the key words "rat model AND (peritoneal metastasis)"*. 23.11.20.
153. Mei LJ, Yang XJ, Tang L, Hassan AH, Yonemura Y, and Li Y, *Establishment and identification of a rabbit model of peritoneal carcinomatosis*

from gastric cancer. BMC Cancer, 2010. **10**: p. 124.

154. Kidd JG and Rous P, *A TRANSPLANTABLE RABBIT CARCINOMA ORIGINATING IN A VIRUS-INDUCED PAPILLOMA AND CONTAINING THE VIRUS IN MASKED OR ALTERED FORM.* J Exp Med, 1940. **71**(6): p. 813-38.
155. Coccolini F, Acocella F, Morosi L, Brizzola S, Ghiringhelli M, Ceresoli M, Davoli E, Ansaloni L, D'Incalci M, and Zucchetti M, *High Penetration of Paclitaxel in Abdominal Wall of Rabbits after Hyperthermic Intraperitoneal Administration of Nab-Paclitaxel Compared to Standard Paclitaxel Formulation.* Pharmaceutical Research, 2017. **34**(6): p. 1180-1186.
156. Pabst R, *The pig as a model for immunology research.* Cell Tissue Res, 2020. **380**(2): p. 287-304.
157. Davigo A, Passot G, Vassal O, Bost M, Tavernier C, Decullier E, Bakrin N, Alyami M, Bonnet JM, Louzier V, Paquet C, Allaouchiche B, Glehen O, and Kepenekian V, *PIPAC versus HIPEC: cisplatin spatial distribution and diffusion in a swine model.* Int J Hyperthermia, 2020. **37**(1): p. 144-150.
158. Giger-Pabst U, Bucur P, Roger S, Falkenstein TA, Tabchouri N, Le Pape A, Lerondel S, Demtröder C, Salamé E, and Ouaissi M, *Comparison of Tissue and Blood Concentrations of Oxaliplatin Administrated by Different Modalities of*

Intraperitoneal Chemotherapy. Ann Surg Oncol, 2019. **26**(13): p. 4445-4451.

159. Reymond MA, Tannapfel A, Schneider C, Scheidbach H, Köver S, Jung A, Reck T, Lippert H, and Köckerling F, *Description of an intraperitoneal tumour xenograft survival model in the pig.* Eur J Surg Oncol, 2000. **26**(4): p. 393-7.
160. Dobson K, Jones S, Liu P, Miao D, Reading L, Shui C, Still K, and Scutt A, *The Advantages and Limitations of Cell Culture as a Model of Bone Formation*. 1998. p. 1-42.
161. Van de Sande L, Rahimi-Gorji M, Giordano S, Davoli E, Matteo C, Detlefsen S, D'Herde K, Braet H, Shariati M, Remaut K, Xie F, Debbaut C, Ghorbaniasl G, Cosyns S, Willaert W, and Ceelen W, *Electrostatic Intraperitoneal Aerosol Delivery of Nanoparticles: Proof of Concept and Preclinical Validation.* Adv Healthc Mater, 2020. **9**(16): p. e2000655.
162. Park S, Park SJ, Lee HS, Ham J, Lee EJ, Kim J, Ryu S, Seol A, Lim W, Lee JC, Song G, Kim HS, and Ko RIATG, *Establishment of an Experimental System for Intraperitoneal Chemotherapy in a Rat Model.* In vivo (Athens, Greece), 2021. **35**(5): p. 2703-2710.
163. Shariati M, Lollo G, Matha K, Descamps B, Vanhove C, Van de Sande L, Willaert W, Balcaen L, Vanhaecke F, Benoit JP, Ceelen W, De Smedt SC, and Remaut K, *Synergy between Intraperitoneal Aerosolization (PIPAC) and*

Cancer Nanomedicine: Cisplatin-Loaded Polyarginine-Hyaluronic Acid Nanocarriers Efficiently Eradicate Peritoneal Metastasis of Advanced Human Ovarian Cancer. ACS Appl Mater Interfaces, 2020. **12**(26): p. 29024-29036.

164. Shariati M, Zhang H, Van de Sande L, Descamps B, Vanhove C, Willaert W, Ceelen W, De Smedt SC, and Remaut K, *High Pressure Nebulization (PIPAC) Versus Injection for the Intraperitoneal Administration of mRNA Complexes.* Pharm Res, 2019. **36**(9): p. 126.
165. Mimouni M, Richard C, Adenot P, Letheule M, Tarrade A, Sandra O, Dahirel M, Lilin T, Lecuelle B, Gélin V, Cohen J, Fauconnier A, Vialard F, Huchon C, and Chavatte-Palmer P, *Pressurized intra-peritoneal aerosol chemotherapy (PIPAC): increased intraperitoneal pressure does not affect distribution patterns but leads to deeper penetration depth of doxorubicin in a sheep model.* BMC Cancer, 2021. **21**(1): p. 461.
166. Tan HL, Kim G, Charles CJ, Li RR, Jang CJ, Shabbir A, Chue KM, Tai CH, Sundar R, Goh BC, Bonney GK, Looi WD, Cheow ES, So JB, Wang L, and Yong WP, *Safety, pharmacokinetics and tissue penetration of PIPAC paclitaxel in a swine model.* Eur J Surg Oncol, 2021. **47**(5): p. 1124-1131.
167. Bellendorf A, Khosrawipour V, Khosrawipour T, Siebigteroth S, Cohnen J, Diaz-Carballo D, Bockisch A, Zieren J, and Giger-Pabst U,

Scintigraphic peritoneography reveals a non-uniform (99m)Tc-Pertechnetat aerosol distribution pattern for Pressurized Intra-Peritoneal Aerosol Chemotherapy (PIPAC) in a swine model. Surg Endosc, 2018. **32**(1): p. 166-174.

168. Tavernier C, Passot G, Vassal O, Allaouchiche B, Decullier E, Bakrin N, Alyami M, Davigo A, Bonnet JM, Louzier V, Paquet C, Glehen O, and Kepenekian V, *Pressurized intraperitoneal aerosol chemotherapy (PIPAC) might increase the risk of anastomotic leakage compared to HIPEC: an experimental study.* Surg Endosc, 2020. **34**(7): p. 2939-2946.
169. Khosrawipour V, Khosrawipour T, Hedayat-Pour Y, Diaz-Carballo D, Bellendorf A, Böse-Ribeiro H, Mücke R, Mohanaraja N, Adamietz IA, and Fakhrian K, *Effect of Whole-abdominal Irradiation on Penetration Depth of Doxorubicin in Normal Tissue After Pressurized Intraperitoneal Aerosol Chemotherapy (PIPAC) in a Post-mortem Swine Model.* Anticancer Res, 2017. **37**(4): p. 1677-1680.
170. Khosrawipour V, Khosrawipour T, Kern AJ, Osma A, Kabakci B, Diaz-Carballo D, Förster E, Zieren J, and Fakhrian K, *Distribution pattern and penetration depth of doxorubicin after pressurized intraperitoneal aerosol chemotherapy (PIPAC) in a postmortem swine model.* J Cancer Res Clin Oncol, 2016. **142**(11): p. 2275-80.

171. Kakchekeeva T, Demtröder C, Herath NI, Griffiths D, Torkington J, Solaß W, Dutreix M, and Reymond MA, *In Vivo Feasibility of Electrostatic Precipitation as an Adjunct to Pressurized Intraperitoneal Aerosol Chemotherapy (ePIPAC).* Ann Surg Oncol, 2016. **23**(Suppl 5): p. 592-598.
172. Seitenfus R, Ferreira PRW, Santos GOD, Alves RJV, Kalil AN, Barros ED, Glehen O, Casagrande TAC, Bonin EA, and Silva Junior EMD, *A prototype single-port device for pressurized intraperitoneal aerosol chemotherapy. Technical feasibility and local drug distribution.* Acta Cir Bras, 2017. **32**(12): p. 1056-1063.
173. Jung do H, Son SY, Oo AM, Park YS, Shin DJ, Ahn SH, Park do J, and Kim HH, *Feasibility of hyperthermic pressurized intraperitoneal aerosol chemotherapy in a porcine model.* Surg Endosc, 2016. **30**(10): p. 4258-64.
174. Mikolajczyk A, Khosrawipour V, Schubert J, Plociennik M, Nowak K, Fahr C, Chaudhry H, and Khosrawipour T, *Feasibility and Characteristics of Pressurized Aerosol Chemotherapy (PAC) in the Bladder as a Therapeutical Option in Early-stage Urinary Bladder Cancer.* In vivo (Athens, Greece), 2018. **32**(6): p. 1369-1372.
175. Tan HL, Kim G, Charles CJ, Li RR, Jang CJM, Shabbir A, Chue KM, Tai CH, Sundar R, Goh BC, Bonney GK, Looi WD, Cheow ESH, So JBY, Wang L, and Yong WP *Safety, pharmacokinetics and*

tissue penetration of PIPAC paclitaxel in a swine model. European Journal of Surgical Oncology, 2020. DOI: https://doi.org/10.1016/j.ejso.2020.06.031.

176. *PubMed Research with the key words "PIPAC"; "(PIPAC) AND (Doxorubicin)"; "(PIPAC) AND (Cisplatin)"; "(PIPAC) AND (Doxorubicin) AND (Cisplatin)"* 10.02.2021.
177. Sautkin I, Solass W, Weinreich FJ, Königsrainer A, Schenk M, Thiel K, and Reymond MA, *A real-time ex vivo model (eIBUB) for optimizing intraperitoneal drug delivery as an alternative to living animal models.* Pleura Peritoneum, 2019. **4**(3): p. 20190017.
178. Shah S, Chandra A, Kaur A, Sabnis N, Lacko A, Gryczynski Z, Fudala R, and Gryczynski I, *Fluorescence properties of doxorubicin in PBS buffer and PVA films.* Journal of photochemistry and photobiology. B, Biology, 2017. **170**: p. 65-69.
179. Chen NT, Wu CY, Chung CY, Hwu Y, Cheng SH, Mou CY, and Lo LW, *Probing the dynamics of doxorubicin-DNA intercalation during the initial activation of apoptosis by fluorescence lifetime imaging microscopy (FLIM).* PLoS One, 2012. **7**(9): p. e44947.
180. Kauffman MK, Kauffman ME, Zhu H, Jia Z, and Li YR, *Fluorescence-Based Assays for Measuring Doxorubicin in Biological Systems.* Reactive oxygen species (Apex, N.C.), 2016. **2**(6): p. 432-439.

181. Braet H, Rahimi-Gorji M, Debbaut C, Ghorbaniasl G, Van Walleghem T, Cornelis S, Cosyns S, Vervaet C, Willaert W, Ceelen W, De Smedt SC, and Remaut K, *Exploring high pressure nebulization of Pluronic F127 hydrogels for intraperitoneal drug delivery.* Eur J Pharm Biopharm, 2021. **169**: p. 134-143.
182. Tempfer CB, Hilal Z, Dogan A, Petersen M, and Rezniczek GA, *Concentrations of cisplatin and doxorubicin in ascites and peritoneal tumor nodules before and after pressurized intraperitoneal aerosol chemotherapy (PIPAC) in patients with peritoneal metastasis.* Eur J Surg Oncol, 2018. **44**(7): p. 1112-1117.
183. Castagna A, Sautkin I, Weinreich F-J, Lee HH, Königsrainer A, Reymond MA, and Nadiradze G, *Influence of pre-analytical sample preparation on drug concentration measurements in peritoneal tissue: an ex-vivo study.* Pleura and Peritoneum, 2021. **6**(3): p. 131-136.
184. Marple VA, *History of Impactors—The First 110 Years.* Aerosol Science and Technology, 2004. **38**(3): p. 247-292.
185. *Wissenschaftliche Einordnung des DIN-Norm Testverfahrens für Inhalationsgeräte. DIN EN 13544-1:2007+A1:2009*. Europäische Norm zur Ermittlung von Aersosolparametern für Inhalationsgeräte Stand: 2018 [cited 05.02.2022]; Available from: https://www.mpvmedical.com/wp-

content/uploads/2018/09/MPV_STU_DIN-NORM.pdf.

186. Park SJ, Lee EJ, Lee HS, Kim J, Park S, Ham J, Mun J, Paik H, Lim H, Seol A, Yim GW, Shim SH, Kang BC, Chang SJ, Lim W, Song G, Kim JW, Lee N, Park JW, Lee JC, and Kim HS, *Development of rotational intraperitoneal pressurized aerosol chemotherapy to enhance drug delivery into the peritoneum.* Drug Deliv, 2021. **28**(1): p. 1179-1187.

187. Colombo PE, Boustta M, Poujol S, Jarlier M, Bressolle F, Teulon I, Ladjemi MZ, Pinguet F, Rouanet P, and Vert M, *Intraperitoneal administration of novel doxorubicin loaded polymeric delivery systems against peritoneal carcinomatosis: experimental study in a murine model of ovarian cancer.* Gynecol Oncol, 2011. **122**(3): p. 632-40.

188. Cho K, Wang X, Nie S, Chen Z, and Shin DM, *Therapeutic Nanoparticles for Drug Delivery in Cancer.* Clinical Cancer Research, 2008. **14**(5): p. 1310-1316.

189. Castagna A, Zander AJ, Sautkin I, Schneider M, Shegokar R, Königsrainer A, and Reymond MA, *Enhanced intraperitoneal delivery of charged, aerosolized curcumin nanoparticles by electrostatic precipitation.* Nanomedicine (Lond), 2021. **16**(2): p. 109-120.

190. Maguire J, Peng, D. *How to Identify Critical Quality Attributes and Critical Process Parameters*. 2015 [cited 06.02.2022]; Available

from: https://pqri.org/wp-content/uploads/2015/10/01-How-to-identify-CQA-CPP-CMA-Final.pdf.

191. Asano Y, Odagiri T, Oikiri H, Matsusaki M, Akashi M, and Shimoda H, *Construction of artificial human peritoneal tissue by cell-accumulation technique and its application for visualizing morphological dynamics of cancer peritoneal metastasis.* Biochem Biophys Res Commun, 2017. **494**(1-2): p. 213-219.
192. Phamduy TB, Sweat RS, Azimi MS, Burow ME, Murfee WL, and Chrisey DB, *Printing cancer cells into intact microvascular networks: a model for investigating cancer cell dynamics during angiogenesis.* Integr Biol (Camb), 2015. **7**(9): p. 1068-78.
193. Lotti M, Capponi MG, Piazzalunga D, Poiasina E, Pisano M, Manfredi R, and Ansaloni L, *Laparoscopic HIPEC: A bridge between open and closed-techniques.* Journal of minimal access surgery, 2016. **12**(1): p. 86-89.
194. Sigrist RMS, Liau J, Kaffas AE, Chammas MC, and Willmann JK, *Ultrasound Elastography: Review of Techniques and Clinical Applications.* Theranostics, 2017. **7**(5): p. 1303-1329.

8 Declaration of contributions

In this doctoral dissertation the following steps were performed by:

- Study design:

I. Sautkin invented the ex vivo eIBUB model. I.Sautkin and M. Reymond proposed the study design.

- Modeling and manufacturing of the ex vivo eIBUB model:

A list of all components needed for the eIBUB model was drawn up by I. Sautkin and ordered by Dr. F-J Weinreich. Installation of all ex vivo eIBUB model components was performed by I. Sautkin.

- Laboratory experiments:

I. Sautkin performed the setup for the ex vivo eIBUB model and conducted all experiments.

- Experiment data were collected and documented by I. Sautkin. The experiments of this doctoral thesis were replicated from [177].

- Measurement of depth of tissue penetration was performed by Dr. W. Solass and Dr. B. Illing. Histological slides were prepared by the technical assistant A. Hack.
- Preanalytical sample preparation for measurement of drug concentration was provided by Dr. F-J. Weinreich and the analyses themselves were performed in an external laboratory.
- Statistical calculations and data analysis were performed by I. Sautkin.
- Data gathering and analysis were performed by I. Sautkin.
- The work was supervised by Prof. M. Reymond
- The manuscript was written by I. Sautkin and M. Reymond.
- The manuscript was reviewed by M. Reymond
- Academic supervision was by A. Königsrainer

9 Publication

The results of this doctoral thesis were published in the following article:

Sautkin I, Solass W, Weinreich FJ, Königsrainer A, Schenk M, Thiel K, Reymond MA. A real-time *ex vivo* model (eIBUB) for optimizing intraperitoneal drug delivery as an alternative to living animal models. Pleura Peritoneum. 2019 Aug 15;4(3):20190017. doi: 10.1515/pp-2019-0017. PMID: 31667331; PMCID: PMC6812219.

10 Acknowledgments

I would like to thank my supervisor Prof. Marc Andre Reymond for allowing me to join his team, for his research support and for his review of my doctoral dissertation. It was a pleasure to meet him and I learned a great deal from him.

I would also like to thank:

- Prof. Alfred Königsrainer for academic supervision,
- Dr. Frank-Juergen Weinreich for ordering experiment equipment and biopsy preparation,
- Dr. Wiebke Solass, Dr. Barbara Illing, and Anita Hack for qualitative biopsy analyses,
- Dr. Ranjita Sahoo for timely comments and guidance,

- Michaela Weiss-Klemm for organizational support,
- Verena Schlaich for personal inspiration.

Finally, I would like to thank my family for their constant support, care, and the results that we have achieved.